

STELLAR STRUCTURE AND EVOLUTION: DEDUCTIONS FROM HIPPARCOS

Yveline Lebreton

Observatoire de Paris, DASGAL-UMR CNRS 8633, Place J. Janssen, 92195 Meudon, France

e-mail: Yveline.Lebreton@obspm.fr

KEYWORDS: Stars: physical processes, distances, H-R diagram, ages, abundances, Hipparcos

ABSTRACT:

During the last decade, the understanding of fine features of the structure and evolution of stars has become possible as a result of enormous progress made in the acquisition of high-quality observational and experimental data and of new developments and refinements in the theoretical description of stellar plasmas. The confrontation of high-quality observations with sophisticated stellar models has allowed many aspects of the theory to be validated, and several characteristics of stars relevant to Galactic evolution and cosmology to be inferred. This paper is a review of the results of recent studies undertaken in the context of the Hipparcos mission, taking benefit of the high-quality astrometric data it has provided. Successes are discussed, as well as the problems that have arisen and suggestions proposed to solve them. Future observational and theoretical developments expected and required in the field are also presented.

CONTENTS

INTRODUCTION	2
NEW HIGH-ACCURACY OBSERVATIONAL MATERIAL	5
<i>Space Astrometry with Hipparcos</i>	5
<i>Ground-Based Photometry and Spectroscopy</i>	7
RECENT THEORETICAL AND NUMERICAL PROGRESS	11
<i>Microscopic Physics</i>	11
<i>Atmospheres</i>	12
<i>Transport Processes</i>	13
STUDIES OF THE BEST-KNOWN OBJECTS	15
<i>Stars in Binary Systems</i>	15
<i>The Nearest Disk and Halo Stars</i>	17
<i>Stars in Open Clusters</i>	24
RARE, FAINT, SPECIAL, OR INACCESSIBLE OBJECTS	31
<i>Globular Clusters Through Halo Stars</i>	31
<i>Variable Stars</i>	35
<i>White Dwarfs</i>	35
FUTURE INVESTIGATIONS	38
Acknowledgments	40

1 INTRODUCTION

Stars are the main constituents of the observable Universe. The temperatures and pressures deep in their interiors are out of reach for the observer, while the description of stellar plasmas requires extensive knowledge in various domains of modern physics such as nuclear and particle physics, atomic and molecular physics, thermo- and hydrodynamics, physics of the radiation and of its interaction with matter, and radiative transfer. The development of numerical codes to calculate models of stellar structure and evolution began more than forty years ago with the pioneering works of Schwarzschild (1958) and Henyey et al (1959). These programs have allowed at least the qualitative study and understanding of numerous physical processes that intervene during the various stages of stellar formation and evolution.

During the last two decades, observational data of increasingly high accuracy have been obtained as a result of 1) the coming of modern ground-based or space telescopes equipped with high-quality instrumentation and with detectors giving access to almost any possible range of wavelengths and 2) the elaboration of various sophisticated techniques of data reduction. Ground-based astrometry has progressed, while space astrometry was initiated with Hipparcos. In the meantime, CCD detectors on large telescopes opened the era of high-resolution, high signal-to-noise ratio spectroscopy while multi-color filters were designed for photometry. New fields have appeared or are under development, such as helio- and asteroseismology or interferometry. On the other hand, stellar models have been enriched by a continuously improved physical description of the stellar plasma, while the use of increasingly powerful computers has led to a gain in numerical accuracy.

The confrontation of models with observations allows testing and even validation of the input physics of the models if numerous observations of high quality are available. Fundamental returns are expected in many domains that make use of quantitative results of the stellar evolution theory such as stellar, Galactic, and extragalactic astrophysics as well as cosmology. Because of their positions, movements, or interactions with the interstellar medium stars are actors and tracers of the dynamical and chemical evolution of the Galaxy. Astrophysicists aim to determine their ages and chemical compositions precisely. For example, the firm determination of the ages of the oldest stars, halo stars or members of globular clusters, is a long-standing objective because it is one of the strongest constraints for cosmology.

Although great progress has been made, a number of observations cannot be reproduced by stellar models, which raises many questions regarding both the observations and the models. In the last few years, two scientific meetings have been explicitly devoted to unsolved problems in stellar structure and evolution (Noels et al 1995, Livio 2000). A major point of concern is that of transport processes at work in stellar interiors (transport of the chemical elements, angular momentum or magnetic fields by microscopic diffusion and/or macroscopic motions). Observations show that transport processes are indeed playing a role in stellar evolution but many aspects remain unclear (sometimes even unknown) and need to be better characterized. Another crucial point concerns the atmo-

spheres, which link the stellar interior model to the interstellar medium and are the intermediate agent between the star and the observer. Uncertainties and inconsistencies in atmospheric descriptions generate errors in the analysis of observational data and in model predictions.

This paper is the third of the series in ARAA dedicated to the results of the Hipparcos mission; Kovalevsky (1998) presented the products of the mission and the very first astrophysical results obtained immediately after the release of the data, while Reid (1999) reviewed the implications of the Hipparcos parallaxes for the location of the main sequence (MS) in the Hertzsprung-Russell (H-R) diagram, the luminosity calibration of primary distance indicators, and the Galactic distance scale. Also, van Leeuwen (1997) presented the results of the mission, and Baglin (1999) and Lebreton (2000) discussed the impact of Hipparcos data on stellar structure and evolution.

Hipparcos has provided opportunities to study rather large and homogeneous samples of stars sharing similar properties, for instance, in terms of their space location or chemical composition. I review studies based on Hipparcos observations which (1) confirmed several elements of stellar internal structure theory, (2) revealed some problems related to the development of stellar models, and (3) yielded more precise characteristics of individual stars and clusters. In Sections 2 and 3, I discuss the recent observational (including Hipparcos) and theoretical developments from which new studies could be undertaken. In Section 4, I concentrate on the nearest stars, observed with highest precision (A-K disk and halo single or binary field stars, and members of open clusters). In Section 5, I review recent results on variable stars, globular clusters and white dwarfs based on Hipparcos data. The stars considered are mostly of low or intermediate mass, and except for white dwarfs, the evolutionary stages cover the main sequence and subgiant branch. Throughout this paper, I emphasize that the smaller error bars on distances that result from Hipparcos make the uncertainties on the other fundamental stellar parameters more evident; fluxes, effective temperatures, abundances, gravities, masses and radii have to be improved correspondingly, implying in many cases the need for progress in atmospheric description.

2 NEW HIGH-ACCURACY OBSERVATIONAL MATERIAL

This section presents a brief review of Hipparcos results and complementary ground-based or space observations which, if combined, provide very homogeneous and precise sets of data.

2.1 *Space Astrometry with Hipparcos*

The Hipparcos satellite designed by the European Space Agency was launched in 1989. The mission ended in 1993 and was followed by 3 years of data reduction. The contents of the Hipparcos Catalogue (Eur. Space Agency 1997) were described by Perryman et al (1997a). The data were released to the astrophysical community in June 1997. General information on the mission is given in van Leeuwen's (1997) and Kovalevsky's (1998) review papers.

Stars of various masses, chemical compositions and evolutionary stages located either in the Galactic disk or in the halo were observed; this was done systematically to a V-magnitude that depends on the galactic latitude and spectral type of the star, and more generally, with a limit of $V \sim 12.4$ mag. The Hipparcos Catalogue lists positions, proper motions, and trigonometric parallaxes of 117 955 stars as well as the intermediate astrometric data, from which the astrometric solutions were derived; this allows alternative solutions for the astrometric parameters to be reconstructed according to different hypotheses (see van Leeuwen & Evans 1998).

A total of 12 195 double or multiple systems are resolved (among which about 25 % were previously classified as single stars), and 8 542 additional stars are suspected to be non-single. Detailed information on multiple systems, as described by Lindegren et al (1997), can be found in The Double and Multiple System Annex of the Catalogue.

The median accuracy on positions and parallaxes (π) is typically ~ 1 milliarcsecond (1 mas), whereas precisions on proper motions are about 1 mas per yr. Precisions become much higher for bright stars and worsen toward the ecliptic plane and for fainter stars. The astrometric accuracy and formal precision of Hipparcos data have been investigated by Arenou et al (1995) and Lindegren (1995), and discussed by van Leeuwen (1999a): for the Catalogue as a whole, the zero-point error on parallaxes is below 0.1 mas and the formal errors are not underestimated

by more than 10%. After Hipparcos about 5 200 single stars and 450 double (or multiple) stars have parallaxes known with an accuracy σ_π/π better than 5%, 20 853 stars have σ_π/π lower than 10% and 49 333 stars have σ_π/π lower than 20% (Mignard 1997). Martin et al (1997, 1998) and Martin & Mignard (1998) determined the masses of 74 astrometric binaries with accuracies in the range 5-35%. Sderhjelm (1999) obtained masses and improved orbital elements for 205 visual binaries from a combination of Hipparcos astrometry and ground-based observations; among these, 12 (20) systems have mass-errors below 5 (7.5)%.

The Hipparcos Catalogue also includes detailed and homogeneous photometric data for each star, obtained from an average number of 110 observations per star. The broad-band Hipparcos (Hp) magnitude corresponding to the specific pass-band of the instrument spanning the wavelength interval ~ 350 -800 nanometers (see Figure 1 in van Leeuwen et al 1997), is provided with a median precision of 0.0015 mag for Hp < 9 mag. The Johnson V magnitude derived from combined satellite and ground-based observations is given with a typical accuracy of 0.01 mag. The star mapper Tycho had passbands close to the Johnson B and V bands and provided two-color B_T and V_T magnitudes (accuracies are typically 0.014 mag and 0.012 mag for stars with $V_T < 9$).

Hipparcos provided a detailed variability classification of stars (van Leeuwen et al 1997), resulting in 11 597 variable or possibly variable stars. Among these 2 712 stars are periodic variables (970 new) including 273 Cepheids, 186 RR Lyrae, 108 δ Scuti or SX Phoenicis stars, and 917 eclipsing binaries.

Hipparcos was planned more than fifteen years ago, and while its development proceeded, significant progress was made in the derivation of ground-based parallaxes using CCD detectors. Parallaxes with errors less than 1.4 mas have already been obtained for a few tens of stars, and errors are expected to drop to ± 0.5 mas in the years to come (Harris et al 1997, Gatewood et al 1998). In addition, the Hubble Space Telescope (*HST*) Fine Guidance Sensor observations can provide parallaxes down to $V \sim 15.8$ with errors at the 1 mas level (Benedict et al 1994, Harrison et al 1999). However, the distances of a rather small number of stars will be measured by *HST* because of the limited observing time available for astrometry. The enormous advantage of Hipparcos resides in the large number of stars it dealt with, providing homogeneous trigonometric parallaxes that are essentially absolute.

2.2 Ground-Based Photometry and Spectroscopy

The fundamental stellar parameters (bolometric magnitude M_{bol} , effective temperature T_{eff} , surface gravity g , and chemical composition) can be determined from photometry and/or from detailed spectroscopic analysis. However, the determination largely relies on model atmospheres and sometimes uses results of interior models. Direct masses and radii can be obtained for stars belonging to binary or multiple systems. Interferometry combined with distances yields stellar diameters giving direct access to T_{eff} , but still for a very limited number of rather bright stars which then serve to calibrate other methods. The different methods (and related uncertainties) used to determine the fundamental stellar parameters mainly for A to K Galactic dwarfs and subgiants are briefly discussed, and improvements brought by Hipparcos are underlined.

BOLOMETRIC MAGNITUDES. Integration of UBVR_IJHKL photometry gives access to the bolometric flux on Earth F_{bol} , at least for F-G-K stars where most energy is emitted in those bands and which are close enough not to be affected by interstellar absorption; the (small) residual flux, emitted outside the bands, is estimated from model atmospheres. Recently, Alonso et al (1995) applied the method to ~ 100 F-K dwarfs and subdwarfs and obtained bolometric fluxes accurate to about 2% and, as a by-product, empirical bolometric corrections for MS stars.

If F_{bol} and distances are known, M_{bol} can be derived with no need for bolometric correction. The accuracy is then $\sigma_{M_{\text{bol}}} = \log e [(2.5 \frac{\sigma_{F_{\text{bol}}}}{F_{\text{bol}}})^2 + (5 \frac{\sigma_{\pi}}{\pi})^2]^{\frac{1}{2}}$, meaning that if $\frac{\sigma_{F_{\text{bol}}}}{F_{\text{bol}}} \sim 2\%$ then $\sigma_{M_{\text{bol}}}$ is dominated by the parallax error as soon as $\frac{\sigma_{\pi}}{\pi} > 1\%$. In other cases, when the distance is known, M_{bol} is obtained from any apparent magnitude m and its corresponding bolometric correction $BC(m)$, derived from empirical calibrations or from model atmospheres. Up to now Hipparcos magnitudes H_p have not been used extensively, despite their excellent accuracy (0.0015 mag), because of remaining difficulties in calculating $BC(H_p)$ (Cayrel et al 1997a).

EFFECTIVE TEMPERATURES. The InfraRed Flux Method (IRFM; Blackwell et al 1990), applicable to A-K stars proceeds in two steps. First, the stellar angular diameter ϕ is evaluated by comparing the IR flux observed on Earth in a given band to the flux predicted by a model atmosphere calculated with

the observed gravity and abundances and an approximate T_{eff} (the IR flux does not depend sensitively on T_{eff}). Then T_{eff} is obtained from the total (integrated) flux F_{bol} and ϕ . Iteration of the procedure yields a “definite” value of T_{eff} . Using IRFM, Alonso et al (1996a) derived temperatures of 475 F0-K5 stars (T_{eff} in the range 4000-8000K) with internal accuracies of $\sim 1.5\%$. The zero-point of their T_{eff} -scale is based on direct interferometric measures by Code et al (1976), and the resulting systematic uncertainty is $\sim 1\%$. Accuracies of $\sim 1\%$ were obtained by Blackwell & Linas-Gray (1998), who applied IRFM to 420 A0-K3 stars, corrected for interstellar extinction using Hipparcos parallaxes. Both sets of results compare well, with differences below $0.12 \pm 1.25\%$ for the 93 stars in common.

The surface brightness method (Barnes et al 1978) was applied by Di Benedetto (1998) to obtain a (T_{eff} , V-K) calibration. The calibration is based on 327 stars with high-precision K-magnitudes from the Infrared Space Observatory (ISO), Hipparcos V-magnitudes and parallaxes (the latter to correct for interstellar extinction), and bolometric fluxes from Blackwell & Linas-Gray (1998). First, the visual surface brightness $S_V = V + 5 \log \phi$ is calibrated as a function of (V-K) using stars with precise ϕ from interferometry. Then for any star S_V is obtained from (V-K), ϕ from S_V and V, yielding in turn T_{eff} from F_{bol} and ϕ . From the resulting (T_{eff} , V-K) calibration, Di Benedetto derived T_{eff} values of 537 ISO A-K dwarfs and giants with $\pm 1\%$ accuracy. The method produces results in good agreement with those of IRFM and is less dependent on atmosphere models.

Multiparametric empirical calibrations of T_{eff} as a function of the color indices and eventually of metallicity $[\text{Fe}/\text{H}]$ (logarithm of the number abundances of Fe to H relative to the solar value) and gravity can be derived from the empirical determinations of the effective temperatures of the rather nearby stars. In turn, the effective temperature of any star lying in the (rather narrow) region of the H-R diagram covered by a given calibration can easily be derived (see for example Alonso et al 1996b). Empirical calibrations also serve to validate purely theoretical calibrations based on model atmospheres; these latter have the advantage of covering the entire parameter space of the H-R diagram (i.e. wide ranges of color indices, metallicities and gravities; see Section 3.2 later in this article).

Spectroscopic determination of T_{eff} is based on the analysis of chosen spectral lines that are sensitive to temperature; for instance the Balmer lines for stars

with T_{eff} in the interval 5000-8000 K. Because of the present high quality of the stellar spectra, precisions of ± 50 -80 K on T_{eff} , that correspond to the adjustment of the theoretical line profile to the observed one, are commonly found in the literature (Cayrel de Strobel et al 1997b, Fuhrmann 1998). This supposes that theoretical profiles are very accurate, and therefore neglects the model atmosphere uncertainties.

Popper (1998) used detached eclipsing binaries with rather good Hipparcos parallaxes, accurate radii, and measured V-flux to calibrate the radiative flux as a function of (B-V); he found good agreement with similar calibrations based on interferometric angular diameters. From the same data, Ribas et al (1998) derived effective temperatures (this required bolometric corrections) and found them to be in reasonable agreement (although systematically smaller by 2-3%) with T_{eff} derived from photometric calibrations. However the stars are rather distant, which implies rather significant internal errors on M_{bol} and T_{eff} (a parallax error of 10% is alone responsible for a T_{eff} -error of 5%). In Ribas et al's sample, only a few systems have $\sigma_{\pi}/\pi < 10\%$, and because errors on radius, magnitudes, and BC also intervene, only 5 systems have T_{eff} determined to better than 3%.

SURFACE GRAVITIES. If T_{eff} and M_{bol} are known, the radius of the star may be derived from the Stefan-Boltzmann law and the mass estimated from a grid of stellar evolutionary models, yielding in turn the value of g . This method has been applied to a hundred metal-poor subdwarfs and subgiants with accurate distances from Hipparcos (Nissen et al 1997, Fuhrmann 1998, Clementini et al 1999). Nissen et al showed that among the various sources of errors, the error on distance still dominates, but pointed out that if the distance error is lower than 20% then the error on $\log g$ may be lower than ± 0.20 dex.

On the other hand, g can be determined from spectroscopy. Different gravities produce different atmospheric pressures, modifying the profiles of some spectral lines. Two methods have been widely used to estimate g . The first method is based on the analysis of the equation of ionization equilibrium of abundant species, iron, for instance. The iron abundance is determined from FeI lines that are not sensitive to gravity, and then g is adjusted so that the analysis of FeII lines, which are sensitive to gravity, leads to the same value of the iron abundance. The accuracy in $\log g$ is in the range ± 0.1 -0.2 dex (Axer et al 1994).

The second method relies on the analysis of the wings of strong lines broadened by collisional damping, such as Ca I (Cayrel et al 1996) or the Mg Ib triplet (Fuhrmann et al 1997), leading to uncertainties smaller than 0.15 dex. The two methods often produce quite different results, with systematic differences of ~ 0.2 - 0.4 dex, at least when ionization equilibria are estimated from models in local thermodynamical equilibrium (LTE).

Thévenin & Idiart (1999) have studied the effects of departures from LTE on the formation of FeI and FeII lines in stellar atmospheres, and found that modifications of the ionization equilibria resulted from the overionization of iron induced by significant UV fluxes. The nice consequence is that the gravities they inferred from iron ionization equilibrium for a sample of 136 stars spanning a large range of metallicities become very close to gravities derived either from pressure-broadened strong lines or through Hipparcos parallaxes.

ABUNDANCES OF THE CHEMICAL ELEMENTS. The spectroscopic determination of abundances of chemical elements rests on the comparison of the outputs of model atmospheres (synthetic spectra, equivalent widths) with their counterpart in the observed spectra. This requires a preliminary estimate of T_{eff} and g . If high-resolution spectra are used, the line widths are very precise and the internal uncertainty in abundance determinations depends on uncertainties in g and T_{eff} , on the validity of the model atmosphere, and on the oscillator strengths. Error bars in the range ± 0.05 - 0.15 dex are typical (Cayrel de Strobel et al 1997b, Fuhrmann 1998). Also when different sets of $[\text{Fe}/\text{H}]$ determinations are compared, the solar Fe/H ratio used as reference must be considered; values differing by ~ 0.15 dex used to be found in the literature (Axer et al 1994). This has resulted in long-standing difficulties in determining the solar iron abundance from FeI or FeII lines, because of uncertain atomic data. In a recent paper, Grevesse & Sauval (1999) reviewed the problem and opted for a “low” Fe-value, $A_{\text{Fe}} = 7.50 \pm 0.05$ ($A_{\text{Fe}} = \log(n_{\text{Fe}}/n_{\text{H}}) + 12$ is the logarithm of the number density ratio of Fe to H particles), in perfect agreement with the meteoritic value.

Furthermore, if abundances are estimated from model atmospheres in LTE, perturbations of statistical equilibrium by the radiation field are neglected. Thévenin & Idiart (1999) found that in metal-deficient dwarfs and subgiants, the iron overionization resulting from reinforced UV flux modifies the line widths. They obtained differential non-LTE/LTE abundance corrections increasing from 0.0

dex at $[\text{Fe}/\text{H}]=0.0$ to $+0.3$ dex at $[\text{Fe}/\text{H}]= -3.0$. These corrections are indeed supported by the agreement between spectroscopic gravities and “Hipparcos” gravities discussed previously.

Helium lines do not form in the photosphere of low-temperature stars which precludes a direct determination of helium abundance. The calibration of the solar model in luminosity and radius at solar age yields the initial helium content of the Sun (Christensen-Dalsgaard 1982), while oscillation frequencies give access to the present value in the convection zone (Kosovichev et al 1992). In other stars, it is common to use the well-known scaling relation $Y - Y_p = Z \frac{\Delta Y}{\Delta Z}$, which supposes that the helium abundance has grown with metallicity Z from the primordial value Y_p to its stellar birth value Y (Y and Z represent abundances in mass fraction); $\Delta Y/\Delta Z$ is the enrichment factor.

α -element abundances (O, Ne, Mg, Si, S, Ar, Ca, Ti) have now been widely measured in metal-deficient stars. Stars with $[\text{Fe}/\text{H}] \lesssim -0.5$ dex generally exhibit an α -element enhancement with respect to the Sun ($[\alpha/\text{Fe}]$) quite independent of their metallicity (Wheeler et al 1989, Mc William 1997). Recent determinations of $[\alpha/\text{Fe}]$ in 99 dwarfs with $[\text{Fe}/\text{H}] < -0.5$ from high-resolution spectra by Clementini et al (1999) yield $[\alpha/\text{Fe}] = +0.26 \pm 0.08$ dex.

3 RECENT THEORETICAL AND NUMERICAL PROGRESS

Recent developments in the physical description of low and intermediate mass stars are briefly presented.

3.1 Microscopic Physics

The understanding of stellar structure benefited substantially from the complete re-examination of stellar opacities by two groups: the Opacity Project (OP, see Seaton et al 1994) and the OPAL group at Livermore (see Rogers & Iglesias 1992). Both showed by adopting different and independent approaches, that improved atomic physics lead to opacities generally higher than the previously almost “universally” used Los Alamos opacities (Huebner et al 1977). The opacity enhancements reach factors of 2-3 in stellar envelopes with temperatures in the range $10^5 - 10^6$ K. With these new opacities, (1) a number of long-standing problems in stellar evolution have been solved or at least lessened and (2) finer

tests of stellar structure could be undertaken. Since opacity is very sensitive to metallicity, any underlying uncertainty on metallicity may be problematic.

Great efforts have also been invested in the derivation of low-temperature opacities, including millions of molecular and atomic lines and grain absorption that are fundamental for the calculation of the envelopes and atmospheres of cool stars (Kurucz 1991, Alexander & Ferguson 1994).

OP and OPAL opacities have been shown to be in reasonable agreement (Seaton et al 1994, Iglesias & Rogers 1996); and very good agreement between OPAL and Alexander & Ferguson's or Kurucz's opacities is found in the domains where they overlap. Although some uncertainties remain that are difficult to quantify, the largest discrepancies between the various sets of tables do not exceed 20% and are generally well understood (Iglesias & Rogers), making opacities much more reliable today than they were ten years ago.

The re-calculation of opacities required appropriate equations of state (EOS). The MH&D EOS (see Mihalas et al 1988) is part of the OP project, while the OPAL EOS was developed at Livermore (Rogers et al 1996). In the meantime, another EOS was designed to interpret the first observations of very low-mass stars and brown dwarfs (Saumon & Chabrier 1991). OPAL and OP EOS are needed to satisfy the strong helioseismic constraints (Christensen-Dalsgaard & Dppen 1992).

3.2 Atmospheres

Atmospheres intervene at many levels in the analysis of observations (Section 2.2). They also provide external boundary conditions for the calculation of stellar structure and necessary relations to transform theoretical (M_{bol} , T_{eff}) H-R diagrams to color-magnitude (C-M) or color-color planes. Models have improved during the last two decades, and attention has been paid to the treatment of atomic and molecular line blanketing. The original programs MARCS of Gustafsson et al (1975) and ATLAS by Kurucz (1979) evolved toward the most recent ATLAS9 version, appropriate for O-K stars (Kurucz 1993) and NMARCS for A-M stars (see Brett 1995 and Bessell et al 1998). On the other hand; very low-mass stellar atmosphere models were developed; Carbon (1979) and Allard et al (1997) reviewed calculation details and remaining problems (such as incomplete opacity data, poor treatment of convection, neglect of non-LTE effects or assumption of

plane-parallel geometry).

COLOR-MAGNITUDE TRANSFORMATIONS. Different sets of transformations (empirical or theoretical) were used to analyze the “Hipparcos” stars. Empirical transformations have been discussed in Section 2.2. The most recent theoretical transformations are compiled by Bessell et al (1998), who used synthetic spectra derived from ATLAS9 and NMARCS to produce broad-band colors and bolometric corrections for a very wide range of T_{eff} , g and $[\text{Fe}/\text{H}]$ values. These authors found fairly good agreement with empirical relations except for the coolest stars (M dwarfs, K-M giants).

INTERIOR/ATMOSPHERE INTERFACE. The external boundary conditions for interior models are commonly obtained from $T(\tau)$ -laws (τ is the optical depth) derived either from theory or full atmosphere calculation. This method is suitable for low- and intermediate-mass stars (it is not valid for masses below $\sim 0.6 M_{\odot}$, Chabrier & Baraffe 1997). Morel et al (1994) and Bernkopf (1998) focused on the solar case where seismic constraints require a careful handling of external boundary conditions. Morel et al pointed out that homogeneous physics should be used in interior and atmosphere (opacities, EOS, treatment of convection) and showed that the boundary level must be set deep enough, in zones where the diffusion approximation is valid. Bernkopf discussed some difficulties in reproducing Balmer lines related to the convection treatment.

3.3 *Transport Processes*

CONVECTION. 3-D numerical simulations at current numerical resolution are able to reproduce most observational features of solar convection such as images, spectra, and helioseismic properties (Stein & Nordlund 1998). However, the “connection” with a stellar evolution code is not easy, and stellar models still mostly rely on 1-D phenomenological descriptions such as the mixing-length theory of convection (MLT, Böhm-Vitense 1958). The mixing-length parameter α_{MLT} (ratio of the mixing-length to the pressure scale height) is calibrated so that the solar model yields the observed solar radius at the present solar age. The question of the variations of α_{MLT} in stars of various masses, metallicities, and evolutionary stages remains a matter of debate (Section 4). As pointed out by Abbett et al (1997), the MLT can reproduce the correct entropy jump across the superadiabatic layer near the stellar surface, but fails to describe the detailed

depth structure and dynamics of convection zones. Abbett et al found that the solar entropy jump obtained in 3-D simulations corresponds to predictions of the MLT for $\alpha_{\text{MLT}} \approx 1.5$. Ludwig et al (1999) calibrated α_{MLT} from 2-D simulations of compressible convection in solar-type stars for a broad range of T_{eff} and g -values. The solar α_{MLT} inferred from 3-D and 2-D simulations is close to what is obtained in solar model calibration. The α_{MLT} dependence with T_{eff} and g of Ludwig et al can be used to constrain the range of acceptable variations of α_{MLT} in stellar models (see Section 4).

OVERSHOOTING. Penetration of convection and mixing beyond the classical Schwarzschild convection cores (overshooting process) modifies the standard evolution model of stars of masses $M \gtrsim 1.2 M_{\odot}$, in particular the lifetimes (see for instance Maeder & Mermilliod 1981, Bressan et al 1981). The extent of overshooting was estimated for the first time from the comparison of observed and theoretical MS widths of open clusters (Maeder & Mermilliod 1981), which yields an overshooting parameter $\alpha_{\text{ov}} \sim 0.2$ (ratio of overshooting distance to pressure scale height). As discussed in detail by Roxburgh (1997), α_{ov} is still poorly constrained despite significant efforts made to establish the dependence of overshooting with mass, evolutionary stage, or chemical composition (see Section 4). Andersen (1991) first pointed out that the simultaneous calibration of well-known binaries (masses and radii at 1-2%) may provide improved constraints for α_{ov} . A modeling of the sample of the best-known binaries indicates a trend for α_{ov} to increase with mass and suggests a decrease of α_{ov} with decreasing metallicity (Ribas 1999), although a larger sample would be desirable to confirm those trends. Further advances are expected from asteroseismology (Brown et al 1994, Lebreton et al 1995).

DIFFUSION OF CHEMICAL ELEMENTS. Various mixing processes may occur in stellar radiative zones (see Pinsonneault 1997). In low-mass stars, microscopic diffusion due to gravitational settling carries helium and heavy elements down to the center and modifies the evolutionary course as well as the surface abundances. It has been proved that microscopic diffusion can explain the low helium abundance of the solar convective zone derived from seismology (Christensen-Dalsgaard et al 1993). On the other hand, turbulent mixing (resulting, for instance, from hydrodynamical instabilities related to rotation, see Zahn 1992) probably inhibits microscopic diffusion. Richard et al (1996) did not find any

conflict between solar models including rotation-induced mixing (to account for Li and Be depletion at the surface) and microscopic diffusion (to account for helioseismic data). More constraints are required to clearly identify (and quantify the effects of) the various candidate mixing processes; this will be illustrated in the following sections.

4 STUDIES OF THE BEST-KNOWN OBJECTS

Stellar model results depend on a number of free input parameters. Some are observational data (mass, chemical composition and age, the latter for the Sun only), whereas others enter phenomenological descriptions of poorly-known physical processes (mixing-length parameter for convection, overshooting, etc). The model outputs have to be compared with the best available observational data: luminosity, T_{eff} or radius, oscillation frequencies, etc. Numerous and precise observational constraints allow assessment of the input physics or give more precise values of the free parameters. They may reveal the necessity to include processes previously neglected and in the best cases to characterize them.

The model validation rests on (1) the nearest objects with the most accurate observations, (2) special objects with additional information such as stars belonging to binary systems, members of stellar clusters or stars with seismic data, and (3) large samples of objects giving access to statistical studies.

4.1 Stars in Binary Systems

Masses are available for a number of stars belonging to binary systems, allowing their “calibration” under the reasonable assumption that the stars have the same age and were born with the same chemical composition (Andersen 1991, Noels et al 1991). A solution is sought which reproduces the observed positions in the H-R diagram of both stars. Andersen (1991) claimed that the only systems able to really constrain the internal structure theory are those with errors lower than 2% in mass, 1% in radius, 2% in T_{eff} and 25% in metallicity.

However, additional observations may sometimes cast doubts on an observed quantity previously determined with good internal accuracy. This occurred recently for the masses of stars in the nearest visual binary system α Centauri. The system has been widely modeled in the past (Noels et al 1991, Edmonds et

al 1992, Lydon et al 1993, Fernandes & Neuforge 1995) with the objective of getting (among others) constraints on the mixing-length parameter. At that time, the astrometric masses were used (internal error of 1%) but the $[\text{Fe}/\text{H}]$ -value was controversial, leading to various possibilities for α_{MLT} -values. Today the situation is still confused: metallicity is better assessed, but new radial velocity measurements yield masses higher than those derived from astrometry (by 6-7%, Pourbaix et al 1999). The higher masses imply a reduction in age by a factor of 2 and slightly different α_{MLT} -values for the two stars. However, the orbital parallax corresponding to the high-mass “option” is smaller than and outside the error bars of both ground-based and Hipparcos parallax π_{HipP} . Pourbaix et al noted the lack of reliability of π_{HipP} given in the Hipparcos Catalogue, but since then it has been re-determined from intermediate data by Sderhjelm (1999) and is now close to (and in agreement with) the ground-based parallax. More accurate radial velocity measurements are therefore needed to assess the high-mass solution.

Possible variations of α_{MLT} have been investigated through the simultaneous modeling of selected nearby visual binary systems (Fernandes et al 1998, Pourbaix et al 1999, Morel et al 2000). Small variations of α_{MLT} (not greater than ≈ 0.2) in the two components of αCen (Pourbaix et al) and ιPeg (Morel et al) have been suggested. Fernandes et al, who calibrated 4 systems and the Sun with the same program and input physics, found that α_{MLT} is almost constant for $[\text{Fe}/\text{H}]$ in the range $[\text{Fe}/\text{H}]_{\odot} \pm 0.3$ dex and masses between 0.6 and 1.3 M_{\odot} . In this mass range the sensitivity of models to α_{MLT} increases with mass (due to the increase with mass of the entropy jump across the superadiabatic layer) which makes the MS slope vary with α_{MLT} . Also, I estimate from my models that a change of α_{MLT} of ± 0.15 around 1 M_{\odot} translates into a T_{eff} -change of $\sim 40\text{-}55$ K depending on the metallicity. On the other hand, with the solar- α_{MLT} value the MS slope of field stars and Hyades stars is well fitted (Section 4.3). It is therefore reasonable to adopt the solar- α_{MLT} value to model *solar-type stars*. For other stars, the situation is less clear. The calibration of α_{MLT} depends on the external boundary condition applied to the model, itself sensitive to the low-temperature opacities, and on the color transformation used for the comparison with observations. Chieffi et al (1995) examined the MS and red giant branch (RGB) in metal-deficient clusters and suggested a constancy of α_{MLT} from MS

to RGB and a decrease with decreasing Z . They found variations of α_{MLT} with Z of ≈ 0.2 - 0.4 , but these are difficult to assess considering uncertainties in the observed and theoretical cluster sequences. On the other hand, calibration of α_{MLT} with 2-D simulations of convection gives complex results (Freytag & Salaris 1999; Freytag et al 1999). In particular, (1) for solar metallicity, α_{MLT} is found to decrease when T_{eff} increases above solar T_{eff} , and to increase slightly when stars move toward the RGB (by ≈ 0.10 - 0.15) and; (2) α_{MLT} does not vary importantly when metallicity decreases at solar T_{eff} . More work is needed to go into finer details, and other calibrators of α_{MLT} are required, such as binary stars in the appropriate range of mass and with various chemical compositions.

The modeling of a moderately large sample of binaries might give information on the variation of helium Y and age with metallicity Z , of great interest for Galactic evolution studies. The combined results for six binary systems and the Sun with the same program by Fernandes et al (1998) and Morel et al (2000) show a general trend for Y to increase with Z : Y increases from 0.25 to 0.30 (± 0.02) when Z increases from 0.007 to 0.03 (± 0.002). However, the Hyades appear to depart from this tendency (see Section 4.3).

The sample of binaries with sufficiently accurate temperatures and abundances is still too meager to allow full characterization of physical processes. Additional data are needed such as observations of binaries in clusters (see Section 4.3) or asteroseismological measurements.

4.2 The Nearest Disk and Halo Stars

FINE STRUCTURE OF THE H-R DIAGRAM. Highly accurate distances for a rather large number of stars in the solar neighborhood were provided by Hipparcos. This allowed the first studies of the fine structure of the H-R diagram and related metallicity effects to be undertaken.

Among an ensemble of ‘‘Hipparcos’’ F-G-K stars closer than 25 pc, with error on parallax lower than 5%, Lebreton et al (1997b) selected stars with $[\text{Fe}/\text{H}]$ in the range $[-1.0, +0.3]$ from detailed spectroscopic analysis ($\sigma_{[\text{Fe}/\text{H}]} \simeq 0.10$ dex, Cayrel de Strobel et al 1997b), F_{bol} and T_{eff} from Alonso et al (1995, 1996a) with $\frac{\sigma_{F_{\text{bol}}}}{F_{\text{bol}}} \sim 2\%$ and $\frac{\sigma_{T_{\text{eff}}}}{T_{\text{eff}}} \sim 1.5\%$ (see Section 2.2) and not suspected to be unresolved binaries. Figure 1 presents the H-R diagram of the 34 selected stars: the error bars are the smallest obtained for stars in the solar neighborhood ($\sigma_{M_{\text{bol}}}$ are in

the range 0.031-0.095 with an average value $\langle\sigma_{\text{M}_{\text{bol}}}\rangle \simeq 0.045$ mag). The sample is compared with theoretical isochrones derived from standard stellar models in Figure 2. Models cover the entire [Fe/H]-range. They account for an α -element enhancement $[\alpha/\text{Fe}] = +0.4$ dex for $[\text{Fe}/\text{H}] \leq -0.5$ and, for non-solar [Fe/H], have a solar-scaled helium content ($Y = Y_{\text{p}} + Z(\Delta Y/\Delta Z)_{\odot}$). The splitting of the sample into a solar metallicity sample and a moderately metal-deficient one (Figure 2a and b) shows that:

1. The slope of the MS is well reproduced with the solar α_{MLT} ,
2. Stars of solar metallicity and close to it occupy the theoretical band corresponding to their (LTE) metallicity range, while for moderately metal deficient stars there is a poor fit.

In general, stars have a tendency to lie on a theoretical isochrone corresponding to a higher metallicity than the spectroscopic (LTE) value. This trend was already noticed by Axer et al (1995) but it is now even more apparent because of the high accuracy of the data. Helium content well below the primordial helium value would be required to resolve the conflict.

This is exemplified by the star μ Cas A, the A-component of a well-known, moderately metal-deficient binary system that has a well-determined mass (error in mass of 8 per cent). The standard model (Figure 3) is more than 200 K hotter than the observed point and is unable to reproduce the observed T_{eff} even if (reasonable) error bars are considered (Lebreton 2000). On the other hand, the mass-luminosity properties of the star are well reproduced if the helium abundance is chosen to be close to the primordial value, although the error bar in mass is somewhat too large to provide strong constraints.

Several reasons can be invoked to explain the poor fit at low metallicities:

1. *Erroneous temperature-scale.* 3-D model atmospheres could still change the T_{eff} -scale as a function of metallicity (Gustafsson 1998), but with the presently (1-D) available models it seems difficult to increase Alonso et al's (1996a) T_{eff} by as much as 200-300 K. As noted by Nissen (1998), this scale is already higher than other photometric scales, by as much as 100 K. Also, Lebreton et al (1999) verified that spectroscopic effective temperatures lead to a similar misfit.

2. *Erroneous metallicities.* As discussed in Section 2.2, the [Fe/H]-values inferred from model atmosphere analysis should be corrected for non-LTE effects. According to Thévenin & Idiart (1999) no correction is expected at solar metallicity, whereas for moderately metal-deficient stars the correction amounts to ~ 0.15 dex.
3. *Inappropriate interior models.* In low-mass stars, microscopic diffusion by gravitational settling can make helium and heavy elements sink toward the center, changing surface abundances as well as inner abundance profiles. In metal-deficient stars this process may be very efficient for three reasons: (1) densities at the bottom of the convection zone decrease with metallicity, which favors settling; (2) the thickness of the convection zones decreases with metallicity, making the reservoir easier to empty; and (3) metal-deficient generally means older, which implies more time available for diffusion.

The two latter reasons are attractive because they qualitatively predict an increasing deviation from the standard case when metallicity decreases. As shown in Figure 3, a combination of microscopic diffusion effects with non-LTE Fe/H corrections could remove the discrepancy noted for μ Cas A: an increase of [Fe/H] by 0.15 dex produces a rightward shift of 80 K of the standard isochrone, representing about one third of the discrepancy. Additionally, adding microscopic diffusion effects, according to recent calculations by Morel & Baglin (1999), provides a match to the observed positions. Moreover, the general agreement for solar metallicity stars (Figure 2a) should remain: (1) at solar metallicities non-LTE corrections are found to be negligible, and (2) at ages of ~ 5 Gyr chosen as a mean age for those (expectedly) younger stars, diffusion effects are estimated to be smaller than the error bars on T_{eff} (Lebreton et al 1999).

To conclude on this point, the high-level accuracy reached for a few tens of stars in the solar neighborhood definitely reveals imperfections in interior and atmosphere models. It casts doubts on abundances derived from model atmospheres in LTE, and favors models that include microscopic diffusion of helium and heavy elements toward the interior over standard models. Also, diffusion makes the surface [Fe/H]-ratio decrease by ~ 0.10 dex in 10 Gyr in a star like μ Cas (Morel & Baglin 1999), which is rather small and hidden in the observational error bars. In very old, very deficient stars, the [Fe/H]-decrease is expected to

be larger (Salaris et al 2000), which makes the relation between observed and initial abundances difficult to establish. In the future, progress will come from the study of enlarged samples reaching the same accuracies and of the acquisition of additional parameters to constrain the models. The knowledge of masses for several binaries in a narrow mass range but large metallicity range would help to constrain the helium abundances, while access to seismological data for at least one or two stars would help to better characterize mixing processes.

STATISTICAL STUDIES. Complete H-R diagrams of stars of the solar neighborhood have been constructed by adopting different selection criteria, and have been compared to synthetic H-R diagrams based on theoretical evolutionary tracks.

- Schröder (1998) proposed diagnostics of MS overshooting based on star counts in the different regions of the “Hipparcos” H-R diagram of stars in the solar neighborhood ($d < 50\text{-}100$ pc). In the mass range $1.2\text{-}2 M_{\odot}$, convective cores are small, and it is difficult to estimate the amount of overshooting with isochrone shapes. Schröder suggested using the number of stars in the Hertzsprung gap, associated with the onset of H-shell burning, as an indicator of the extent of overshooting around $1.6 M_{\odot}$; the greater the overshooting on the MS, the larger the He-burning core, and in turn the longer the passage through the Hertzsprung gap. Actual star counts favor an onset of overshooting around $\sim 1.7 M_{\odot}$ (no overshooting appears necessary below that mass), which is broadly consistent with other empirical calibrations (MS width, eclipsing binaries), but finer quantitative estimates would require more accurate observational parameters, mainly in T_{eff} and Z .
- Jimenez et al (1998) compared the red envelope of “Hipparcos” subgiants ($\sigma_{\pi}/\pi < 0.15$, $\sigma_{(B-V)} < 0.02$ mag) with isochrones to determine a minimum age of the Galactic disk of 8 Gyr, which is broadly consistent with ages obtained with other methods (white-dwarf cooling curves, radioactive dating, isochrones, or fits of various age-sensitive features in the H-R diagram). The fit is still qualitative: the metallicities of subgiants are unknown because of the inadequacy of model atmospheres in that region. For this reason, Jimenez et al investigated the isochrones in other regions, MS and clump

(He core burning). They calculated the variations with mass of the clump position for a range of metallicities in the disk, and showed that stars with masses from 0.8 to 1.3 M_{\odot} (ages from 2 to 16 Gyr) all occupy a well-defined vertical branch, the red-edge of the clump. The color of this border line is sensitive to metallicity, which makes it a good metallicity indicator in old metal-rich populations.

- Ng & Bertelli (1998) revised the ages of stars of the solar neighborhood and derived corresponding age-metallicity and age-mass relations. Fuhrmann (1998) combined the $[\text{Mg}/\text{H}]-[\text{Fe}/\text{H}]$ relation with age and kinematical information to distinguish thin and thick disk stars. Several features seem to emerge from these studies: (1) no evident age-metallicity relation exists for the youngest (< 8 Gyr) thin-disk stars; some of them are rather metal-poor, and super metal-rich stars appear to have been formed early in the history of the thin disk; (2) there is an apparent lack of stars in the age-interval 10-12 Gyr which is interpreted by Fuhrmann as a signature of the thin-disk formation; and (3) beyond 12 Gyr there is a slight decrease of metallicity with increasing age for stars of the thick disk; some of them are as old as halo stars. To assess these suggestions and to assist progress in the understanding of the Galactic evolution scenario (see Fuhrmann 1998 for details), enlarged stellar samples and further improvements on age determinations are of course required.

THE SUBDWARF/SUBGIANT SEQUENCE. Hipparcos provided the very first high-quality parallaxes for a number of halo stars. Age determinations of the local halo could be undertaken, as well as comparisons with globular cluster sequences.

Among a large sample of Population II Hipparcos halo subdwarfs, Cayrel et al (1997b) extracted the best-known stars with criteria similar to those adopted by Lebreton et al (1999) for disk stars. Stars were corrected for reddening, excluding stars with $E(\text{B}-\text{V}) > 0.05$. Prior to Hipparcos, only 5 halo stars had parallax errors smaller than 10%; now there are 17, which represents sizeable progress. The halo stars are plotted in Figure 4; subdwarfs but also subgiants are present, delineating an isochrone-like shape with a turn-off region.

To make a first estimate of the age of the local halo, Cayrel et al kept 13 stars with the lowest error bars and spanning a narrow metallicity range ($[\text{Fe}/\text{H}] = -$

1.5±0.3), the most commonly found in the halo (Figure 5). They found that halo stars, like disk stars, are colder than the theoretical isochrone corresponding to their metallicity. The misfit was also noted by Nissen et al (1997) and Pont et al (1997) in larger samples of halo stars. The discrepancy amounts to 130 to 250 K depending on the metallicity, and comparisons indicate that it is independent of the particular set of isochrones used. Again, non-LTE corrections leading to increased [Fe/H]-values ($\Delta[\text{Fe}/\text{H}] = +0.2$ for $[\text{Fe}/\text{H}] \sim -1.5$ according to Thévenin & Idiart 1999), added to the effects of microscopic diffusion, can be invoked to reduce the misfit. Figure 5a compares Cayrel et al's sample with standard isochrones by PA Bergbusch & DA Vandenberg (2000, in preparation), showing that the subdwarf main sequence cannot be reproduced by isochrones computed with the LTE [Fe/H]-value, but increasing the metallicity (to mimic non-LTE corrections) improves the fit. Figure 5b compares the halo sequence with Proffitt & Vandenberg's (1991) isochrones that include He sedimentation. Microscopic diffusion makes the isochrones redder, modifies their shape, and predicts a lower turn-off luminosity: the best fit with the observed sequence is achieved for an age smaller by 0.5-1.5 Gyr than that obtained without diffusion. Models by Castellani et al (1997) show that, if sedimentation of metals is also taken into account, including its effects on the matter opacity, the isochrone shift is smaller than the shift obtained with He diffusion only.

Cayrel et al (1997b) and Pont et al (1997) estimated the local halo to be 12-16 Gyr old (from standard isochrones). To improve the precision more stars with accurate parallaxes are required. Subgiants are about 100 times rarer than subdwarfs, and we have only two subgiants with $\sigma_\pi/\pi < 12.5\%$ (and no subgiant with $\sigma_\pi/\pi < 5\%$). After Hipparcos the position of the subgiant branch is still poorly determined, which limits the accuracy on the age determination of the halo stars.

THE ZAMS POSITIONS. The sample made of Hipparcos disk and halo stars spans the whole Galactic metallicity range. Figure 6 shows the non-evolved stars ($M_{\text{bol}} > 5.5$) of Figure 1 and Figure 4 along with standard isochrones of various metallicities and solar-scaled helium ($(\Delta Y/\Delta Z)_\odot = 2.2$). It allows a discussion of the position of the zero age main sequence (ZAMS) as a function of metallicity and implications for the unknown helium abundances.

- *MS width.* Although stars generally do not lie where predicted, in particular

at low metallicities, the observational and theoretical MS widths are in reasonable agreement for $\Delta Y/\Delta Z = 2.2$. This qualitative agreement is broadly consistent with $\Delta Y/\Delta Z$ ratio of $\simeq 3 \pm 2$ derived from similar measures of the lower MS width by Pagel & Portinari (1998) and the lower limit $\Delta Y/\Delta Z \gtrsim 2$ obtained by Fernandes et al (1996) from pre-Hipparcos MS. It also agrees with extragalactic determinations (see Izotov et al 1997) or nucleosynthetic predictions.

- *Helium abundance at solar metallicities.* It can be noted from Figure 6 that there are 4 stars with Fe/H close to solar on the $[\text{Fe}/\text{H}] = 0.3$ isochrone. Non-LTE $[\text{Fe}/\text{H}]$ -corrections are negligible at solar metallicity. Microscopic diffusion may produce a shift in the H-R diagram: for a $0.8 M_{\odot}$ star of solar Fe/H at 5 Gyr the shift is small and comparable to the observational error bars (but it increases with age). These disk stars are not expected to be very old and the shift could instead indicate that their He-content is lower than the solar-scaled value. Calibration of individual objects and groups with metallicities close to solar indicate an increase of helium with metallicity corresponding to $\Delta Y/\Delta Z \simeq 2.2$ from the Sun (Lebreton et al 1999) and $\Delta Y/\Delta Z \simeq 2.3 \pm 1.5$ from visual binaries (Fernandes et al 1998) but exceptions are found, such as in the (rather young) Hyades which, although metal-rich ($[\text{Fe}/\text{H}] = 0.14$), appear to have a solar or even slightly sub-solar helium content with $\Delta Y/\Delta Z \simeq 1.4$ (Perryman et al 1998). Going into finer resolution would clearly require more complete data including masses for enlarged samples of non-evolved stars.
- *Position of metal-deficient stars.* Very few metal-deficient stars have accurate positions in the non-evolved part of the H-R diagram: a gap appears for $[\text{Fe}/\text{H}] \in [-1.4, -0.3]$ and only 4 subdwarfs are found below $[\text{Fe}/\text{H}] \sim -1.4$. The empirical dependence of the ZAMS location with metallicity is impossible to establish for these stars, which are expected to have practically primordial helium contents. This adds to difficulties in estimating the distances of globular clusters (Eggen & Sandage 1962; Sandage 1970, 1983; Chaboyer et al 1998).

4.3 Stars in Open Clusters

Hipparcos observed stars in all open clusters closer than 300 pc and in the richest clusters located between 300 and 500 pc providing valuable material for distance scaling of the Universe and for studies of kinematical and chemical evolution of the Galaxy. The absolute cluster sequences in the H-R diagram may be constructed directly from Hipparcos distances independently of any chemical composition consideration. Each sequence covers a large range of stellar masses and contains stars which can reasonably be considered to be born at the same time with similar chemical composition. Several clusters provide tests of the internal structure models for a wide range of initial parameters, in particular for different metallicities.

THE HYADES. Obtaining high-quality astrometric data for the Hyades has been crucial, for it is the nearest rich star cluster, used to define absolute magnitude calibrations and the zero-point of the Galactic and extragalactic distance scales. Individual distances (mean accuracy of 5%) and proper motions were given by Hipparcos, providing a consistent picture of the Hyades distance, structure and dynamics (Perryman et al 1998). The recent determinations of the Hyades distance modulus ($m - M$) are all in very good agreement while the internal accuracy was largely improved with Hipparcos:

- ground-based: $m - M = 3.32 \pm 0.06$ mag (104 stars, van Altena et al 1997b)
- *HST* : $m - M = 3.42 \pm 0.09$ mag (7 stars, van Altena et al 1997a)
- Hipparcos: $m - M = 3.33 \pm 0.01$ mag (134 stars within 10 pc of the cluster center, Perryman et al 1998)
- statistical parallaxes based on Hipparcos proper motions: $m - M = 3.34 \pm 0.02$ mag (43 stars, Narayanan & Gould 1999a who also showed that the systematic error on the parallaxes toward the Hyades is lower than 0.47 mas).

Greatly improved precision is seen in the H-R diagrams built with Hipparcos data combined with the best ground-based observations (Perryman et al 1998):

- Figure 7 shows 40 stars with T_{eff} and $[\text{Fe}/\text{H}] = 0.14 \pm 0.05$ from detailed spectroscopic analysis delineating the lower part of the observational MS of the cluster (Cayrel de Strobel et al 1997a).

- Figure 8 is the whole H-R diagram in the $(M_V, B-V)$ plane for 69 cluster members. Known or suspected binaries, variable stars, and rapid rotators have been excluded (Perryman et al 1998). Also, Dravins et al (1997) derived dynamical parallaxes for the Hyades members from the relation between the cluster space motion, the positions and the projected proper motions; these parallaxes are more precise (by a factor of about 2) than those directly measured by Hipparcos, yielding in turn a remarkably well-defined MS sequence in the H-R diagram, narrower than that given in Figure 8 (see Figure 2 in Dravins et al 1997).
- Figure 9 shows the empirical mass-luminosity (M-L) relation drawn from the (very accurate) masses of 5 binary systems (see caption). Nine of the stars are MS stars.

Comparisons with theoretical models yield some of the cluster characteristics (Lebreton et al 1997a, Perryman et al 1998, Lebreton 2000):

1. The comparison of the lowest part of the MS (Figure 7), representing the non-evolved stars, with theoretical ZAMS corresponding to the mean observed $[Fe/H]$ yields the initial cluster helium content $Y_H=0.26\pm 0.02$ and metallicity $Z_H=0.024\pm 0.04$. Metallicity is the dominant source of the uncertainty on Y .
2. The comparison of the whole observed sequence with model isochrones yields the cluster age. Figure 8 shows that the optimum fit is achieved with an isochrone of 625 ± 50 Myr, $Y_H=0.26$, $Z_H=0.024$ and including overshooting. The turn-off region (which in the Hyades corresponds to the instability strip of δ Scuti stars) is rather well represented by the 625 Myr isochrone (see also Antonello & Pasinetti Fracassini 1998). The quoted uncertainty on age only includes the contribution from visual fitting of the isochrones. Additional errors on age result from unrecognized binaries, rotating stars, color calibrations and bolometric corrections, and from theoretical models in particular through the parameterization of overshooting (Lebreton et al 1995). It is therefore reasonable to give an overall age uncertainty of at least 100 Myr.
3. In Figure 9a the observed M-L relation is compared with the theoretical isochrone of 625 Myr, $Y_H = 0.26$, $Z_H = 0.024$, showing an excellent agree-

ment. The lower part of the relation is defined by the very accurate masses of the two components of vB22. This system gives additional constraints on the Y_H -value derived from ZAMS calibration. Figure 9b illustrates how the positions of the two vB22 components may be used to constrain Y_H in the whole metallicity range allowed by observations, $[\text{Fe}/\text{H}]=0.14\pm 0.05$ (see also Lebreton 2000).

Furthermore, in the turn-off region of the Hyades, 5 δ Scuti stars are found that are quite rapid rotators ($v_e \sin i$ in the range 80-200 km.s^{-1} , see Antonello & Pasinetti Fracassini 1998). From the measurement and analysis of their oscillation frequencies and the identification of the corresponding modes by means of models (of same age and chemical composition), we should be able to derive the inner rotation profile and learn about the size of convective cores and transport processes at work in the interiors (Goupil et al 1996, Michel et al 1999). For instance, the rotation profile is related to the redistribution of angular momentum by internal motions which could be generated by meridional circulation and shear turbulence in a rotating medium (see Zahn 1992). On the other hand, such motions might induce internal mixing, and as shown by Talon et al (1997), in the H-R diagram rotational effects “mimic” overshooting (for instance, in a star of $9 M_\odot$, a rotational velocity of $\sim 100 \text{ km.s}^{-1}$ is equivalent to an overshooting of $\alpha_{\text{ov}} \sim 0.2$).

The study and intercomparison of accurate observations of the non-pulsating and pulsating stars located in the instability strip should clearly provide deeper insight into the internal structure and properties of stars of the Hyades cluster. However, such analysis has to integrate the various complications related to rotation, such as the displacements in any photometric H-R diagram by amounts depending on the equatorial velocity and inclination (Maeder & Peytremann 1972, Pérez-Hernández et al 1999) or the splitting of oscillation frequencies, which has to be considered in the mode identification.

THE PLEIADES AND OTHER OPEN CLUSTERS. The membership of stars in nine clusters closer than 300 pc was carefully assessed by van Leeuwen (1999a) and Robichon et al (1999a). Robichon et al also studied nine rich clusters within 500 pc with more than 8 members and 32 more distant clusters. For clusters closer than 500 pc, the accuracy on the mean parallax is in the range 0.2-0.5 mas and the accuracy on the mean proper motions is of the order of 0.1 to 0.5 mas

per year. Results from the two groups are in very good agreement. Platais et al (1998) looked for (new) star clusters in Hipparcos data and found one new, a nearby cluster in Carina (d=132 pc) with 7 identified members.

In order to obtain an optimal mean parallax with correct error estimates, van Leeuwen (1999a) and Robichon et al (1999a) worked with the Hipparcos intermediate data corresponding to each cluster, parallax and proper motion of the cluster center, and position of each cluster member, instead of making a straight average of the parallaxes of the cluster members. Stars in open clusters are located within a few degrees on the sky and hence were often observed in the same field of view of the satellite. A combined solution can be obtained from intermediate data, which allows angular correlations to be taken into account and the resulting parallax errors to be minimized (van Leeuwen & Evans 1998; van Leeuwen 1999a, b; Robichon et al 1999a).

Mermilliod et al (1997), Robichon et al (1997), and Mermilliod (2000) compared the sequences of the various clusters in C-M diagrams derived from different photometric systems, and found puzzling results that are at odds with the common idea that differences in metallicity fully explain the relative positions of the non-evolved parts of the MS of different clusters:

- Some clusters have different metallicities but define the same main sequence in the (M_V , B-V) plane (Praesepe, Coma Ber, α Per, Blanco 1). For instance, Coma Ber has a quasi-solar metallicity while its sequence is similar to that of the Hyades, or of the metal-rich Praesepe.
- Some clusters sequences (Pleiades, IC 2391 and 2602) are abnormally faint with respect to others, for instance Coma Ber. The metallicity of the Pleiades as determined from spectroscopy is almost solar, and similar to that of Coma Ber, but the Pleiades sequence lies (unexpectedly) ~ 0.3 - 0.4 mag below the Praesepe, Coma Ber, or Hyades sequence.
- Van Leeuwen (1999a, b) even suggested a possible (although unexpected) correlation between the age of a cluster and its position in the H-R diagram.

Prior to Hipparcos, precise trigonometric parallaxes had not been obtained for clusters except the Hyades. Distances to open clusters were evaluated through the main sequence fitting technique: the non-evolved part of the (observed) cluster sequence was compared to the non-evolved part of the (absolute) lower MS

(ZAMS) of either (1) theoretical isochrones, (2) field stars or (3) Hyades after a possible correction of chemical composition differences. The magnitude differences between absolute and apparent ZAMS directly yielded the distance modulus of the cluster.

The Hipparcos distances to the 5 closest open clusters (Hyades, Pleiades, α Per, Praesepe, and Coma Ber) can be compared to those recently derived from MS fitting by Pinsonneault et al (1998); they compared theoretical isochrones, translated into the C-M plane by means of Yale color calibrations, to observational data both in the (M_V , B-V) and (M_V , V-I) planes. The B-V color indice is more sensitive to metallicity than V-I (Alonso et al 1996b), so Pinsonneault et al derived as a by-product the value of the metallicity that gives the same distance modulus in the two planes and compared it to spectroscopic determinations. They judged their distance moduli to be in good agreement with Hipparcos results except for the Pleiades and Coma Ber. For Coma Ber, the problem could result from the old VRI colors used. For the Pleiades the discrepancy with Hipparcos amounts to 0.24 mag, and the [Fe/H]-value derived from MS fitting in the two color planes agrees with the spectroscopic determination of Boesgaard & Friel (1990), [Fe/H]= -0.034 ± 0.024 , although values in the range -0.03 to +0.13 can be found in the literature. In fact, with that metallicity the Hipparcos sequence of the Pleiades could be reproduced by classical theoretical models, provided they have a high helium content. The exact value depends on the model set and its input physics: Pinsonneault et al found $Y=0.37$, Belikov et al (1998) found $Y=0.34$ but for [Fe/H]=0.10 and I find $Y \sim 0.31$. In any case, high helium content is only marginally supported by observations (Nissen 1976). Pinsonneault et al examined other possible origins of the discrepancy (erroneous metallicity, age-related effects, reddening) and concluded that none of them is likely to be responsible for the Pleiades discrepancy.

In parallel, Soderblom et al (1998) looked for young solar-type stars appearing as (anomalously) faint as the Pleiades. They found 50 field stars expected to be young (i.e. showing activity from Ca II H and K lines), but none of them lies significantly below the ZAMS. They also examined the subluminous stars observed by Hipparcos: they chose six stars among those lying well below the ZAMS, measured their spectroscopic metallicities, and found them to be metal-deficient with respect to the Sun with, in addition, kinematics typical of stars of

a thick disk or halo population.

Soderblom et al and Pinsonneault et al concluded that, taking the Hipparcos results for the Pleiades at face value, it would be abnormal not to find stars similar to the Pleiades in the field. They inferred that the distance obtained from multi-color MS fitting is correct and accurate to about 0.05 mag, and concluded that the distance to Pleiades obtained from the analysis of Hipparcos data is possibly wrong at the 1 mas level, which is greater than the mean random error. They invoked statistical correlations between right ascension and parallax ($\rho_{\alpha \cos \delta}^{\pi}$) arising from the non-uniform distribution of Hipparcos observations over time (and in turn along the parallactic ellipse) which affects all stars, including clusters. Pinsonneault et al noted that in the Pleiades the brightest stars (1) are highly concentrated near the cluster center and are therefore subject to spatial correlations which gives them nearly the same parallax, (2) have smaller σ_{π} than fainter stars which gives them more weight in the mean parallax, and (3) are those which have the highest values of $\rho_{\alpha \cos \delta}^{\pi}$ and also the highest parallaxes in the Hipparcos Catalogue. They suggest that the “true” parallax (close to that obtained through MS fitting) is obtained if the brightest stars with high $\rho_{\alpha \cos \delta}^{\pi}$ are excluded from the calculation.

Narayanan & Gould (1999b) determined the parallaxes of the Pleiades stars by means of Hipparcos proper motions. The resulting distance modulus has a rather large error bar ($m - M = 5.58 \pm 0.18$ mag), but it is in disagreement with that derived directly from Hipparcos parallaxes ($m - M = 5.36 \pm 0.07$ mag), and in agreement with that obtained through MS fitting ($m - M = 5.60 \pm 0.05$ mag). Narayanan & Gould also argue that the differences between the Hipparcos trigonometric parallaxes and the parallaxes derived from Hipparcos proper motions reflect spatial correlations over small angular scales with an amplitude of up to 2 mas.

Robichon et al (1999a, b) and van Leeuwen (1999b) have subsequently derived more reliable distance estimates to these clusters and performed tests that do not support Pinsonneault et al’s conclusion. The difference between Hipparcos and MS fitting distance moduli is small for the Hyades (0.01 mag), whereas for other clusters it ranges from -0.17 mag (α Per) to +0.24 mag (Pleiades). In fact, except for the Hyades, the difference is always larger than the error on MS fitting distance modulus (0.05 mag). Robichon et al showed that while the solution

proposed by Pinsonneault et al improves the situation for the Pleiades, it would introduce new difficulties for Praesepe. By means of Monte-Carlo simulations of the Pleiades stars, they showed that the mean value of the Pleiades parallax does not depend on the correlations $\rho_{\alpha \cos \delta}^{\pi}$. They also carefully examined distant stars and clusters with high $\rho_{\alpha \cos \delta}^{\pi}$. Through these tests, Robichon et al made the Hipparcos distance to Coma Ber or Pleiades more secure, and did not find any obvious bias on the parallax resulting from a correlation between right ascension and parallax, either for stars within a small angular region or for the whole sky.

On the other hand, distances from MS fitting could be subject to higher error bars than quoted by Pinsonneault et al. They depend on reddening and on transformations from the $(M_{\text{bol}}, T_{\text{eff}})$ to the C-M plane if theoretical ZAMS are used as reference (or on metallicity corrections if empirical ZAMS are compared). Robichon et al (1999b) compared solar ZAMS from Pinsonneault et al to those I calculated both in the theoretical and in the $(M_V, B-V)$ planes. They showed that while the two ZAMS are within 0.05 mag in the theoretical H-R diagram, they differ by 0.15-0.20 mag in the range $B-V=0.7-0.8$ in the $(M_V, B-V)$ plane, simply because different C-M transformations have been applied. Also, MS fitting often relies on rather old and inhomogeneous color sources (in the separate Johnson and Kron-Eggen RI systems) requiring transformations to put all data on the same (Cape-Cousins system) scale. It would therefore be worthwhile to verify the quality and precision of these data by making new photometric measurements of cluster stars.

Let us come back to the difficult question of metallicity. As pointed out by Mermilliod et al (1997), photometric and spectroscopic approaches may produce quite different results. Metallicities have been derived recently by M Grenon (1998, private communication) from large sets of homogeneous observations in the Geneva photometric system. He obtained $[\text{Fe}/\text{H}]=-0.112\pm 0.025$ for the Pleiades (quite different from published spectroscopic values) and $[\text{Fe}/\text{H}]=0.170\pm 0.010$ and 0.143 ± 0.008 for Praesepe and the Hyades respectively (both in agreement with spectroscopy). The observed cluster sequences obtained with Hipparcos distances for the three clusters can be roughly reproduced by theoretical models computed with the photometric metallicities (and allowing for small variations of the helium content around the solar-scaled value) and transformed to the C-M plane according to the Alonso et al (1996b) and Bessell et al (1998) calibrations

(Robichon et al 1999b).

In conclusion, we point out that a detailed study of the fine structure of the H-R diagram of the Pleiades (and other clusters) requires supplementary observations (colors and abundances) and further progress in model atmospheres. Today there is no obvious solid argument against the published Hipparcos distances. In order to identify and understand the remaining discrepancies with stellar models, the entire set of observed clusters has to be considered (van Leeuwen 1999a). Furthermore, not only the positions of the sequences in the H-R diagram but also the density of stars along them have to be intercompared. For instance, the luminosity function of young clusters exhibits a particular feature (local peak followed by dip) that is interpreted as a signature of pre-MS stars and might provide information on the initial mass function and stellar formation history (see the study of the Pleiades by Belikov et al 1998). On the other hand, since the error bars on luminosity are now small with respect to errors on color indices, stronger constraints are expected from the mass-luminosity relation, as in the Hyades. Observations of binaries in clusters are urgently needed and there is hope to detect them in the future, for, as pointed out by Soderblom et al, the difficult detection and measurement of visual binary orbits in the Pleiades is within the capabilities of experiments on board *HST*.

5 RARE, FAINT, SPECIAL, OR INACCESSIBLE OBJECTS

5.1 Globular Clusters Through Halo Stars

Globular clusters were beyond the possibilities of Hipparcos, but the knowledge of distances to nearby subdwarfs gave distance estimates to a few of them through the MS fitting technique (Sandage 1970; Reid 1997, 1998; Gratton et al 1997; Pont et al 1997, 1998; Chaboyer et al 1998), comparing the non-evolved part of the (absolute) subdwarf main-sequence to the non-evolved part of the (observed) globular cluster sequence. Although simple, the technique has to be applied with caution:

- Only halo subdwarfs and globular clusters with the most precise data should be retained. Abundances should be accurate and on a consistent scale. Globular cluster abundances are usually determined only for giants, while recent preliminary values have been obtained for subgiants in M92 (King et

al 1998). Abundance comparisons between (1) field and cluster stars and (2) dwarfs and giants have shown sometimes puzzling differences (King et al 1998, Reid 1999). Questions have been raised as to whether they are primordial or appear during evolution, but definite answers clearly require better spectra for all types of stars as well as spherical model atmospheres with better treatment of convection. The globular cluster sequence should be determined from good photometry well below the MS turn-off, and the correction for interstellar reddening has to be well estimated. Very few halo stars have parallaxes accurate enough to fix precisely the position of the ZAMS (Section 4.2).

- Biases (see e.g. Lutz & Kelker 1973; Hanson 1979; Smith 1987) resulting from the selection of the sample in apparent magnitude, parallax, and metallicity, have to be corrected for (Pont et al 1998, Gratton et al 1997); alternatively, samples free of biases must be selected, which implies retaining the very nearby stars with highly accurate parallaxes (Chaboyer et al 1998, Brown et al 1997).
- Globular cluster sequence and halo sequence should (ideally) have similar *initial* chemical compositions. Because of the small number of subdwarfs in each interval of metallicity, it is not possible to properly establish the variation of the observed ZAMS position with metallicity, and to correct for chemical composition differences between globular clusters and subdwarfs empirically. Chaboyer et al (1998) found it safer to limit the method to globular clusters that have their equivalent in the field with the same $[\text{Fe}/\text{H}]$ and $[\alpha/\text{Fe}]$ content. Gratton et al (1997) and Pont et al (1998) applied theoretical color corrections to the subdwarf data to account for metallicity differences with globulars. In addition, element sedimentation might introduce further difficulties, as already mentioned in Section 4.2. As pointed out by Salaris & Weiss (2000), the present surface chemical composition of field subdwarfs no more reflects the initial one if microscopic diffusion has been efficient during evolution, while, in globular cluster giants which have undergone the first dredge-up, the chemical abundances have been almost restored to the initial ones.
- Unresolved known or suspected binaries can introduce errors in the defi-

dition of the ZAMS position. Chaboyer et al and Gratton et al excluded them whereas Pont et al applied an average correction of 0.375 mag on their position, a procedure that has been criticized by Chaboyer et al and Reid (1998).

- Evolved stars have to be excluded (there is no certainty that globular clusters and halo dwarfs have exactly the same age). From theoretical models it is estimated that stars fainter than $M_V \simeq 5.5$ are essentially unevolved.

The number of globular clusters studied by the different authors varies because of the different criteria and techniques chosen to select the subdwarfs samples. Nevertheless they all agree on the general conclusion that globular cluster distances derived from MS fitting are larger by $\sim 5-7\%$ than was previously found. Chaboyer (1998) calculated an average of distances to globular clusters obtained with different methods (MS fitting, astrometry, white dwarf sequence fitting, calibration of the mean magnitudes of RR Lyrae stars in the Large Magellanic Cloud, comparison with theoretical models of horizontal branch stars, statistical parallax absolute magnitude determinations of field RR Lyrae from the Hipparcos proper motions, etc) and noted that the distance scale is larger (by 0.1 mag) than his pre-Hipparcos reference.

It is worth pointing out that the statistical parallax method alone favors a shorter distance scale (by ≈ 0.3 mag with respect to MS fitting result). As reviewed by Layden (1998) and by Reid (1999), the statistical parallax method was applied by independent groups who found concordant results. However, the absolute magnitudes $M_V(\text{RR})$ of the halo RR Lyrae derived from the statistical parallax method (on the basis of Hipparcos proper motions and of radial velocities) are also ≈ 0.3 mag fainter than the magnitudes obtained through a method directly based on Hipparcos parallaxes (Groenewegen & Salaris 1999); these latter being in turn in good agreement with the MS fitting result. As discussed thoroughly by Reid (1999), there are several difficulties related to the $M_V(\text{RR})$ -calibration and to its comparison with other distance calibrations that still hinder the coherent and homogeneous understanding of the local distance scale.

In Caputo's (1998) and Reid's (1999) reviews the ages of globulars are discussed. After Hipparcos, ages of globular clusters are reduced by typically 2-3 Gyr, because of both larger distances and improvements in the physics of the

models, mainly in the equation of state and in the consideration of microscopic diffusion. Present ages are now in the range 10-13 Gyr, which can be compared to the previous interval of 13-18 Gyr (see Vandenberg et al's review, 1996).

Chaboyer et al (1998) claimed that the (theoretical) absolute magnitude M_V and lifetimes of stars at the MS turn-off (T-O) in globular clusters are now well understood, since the physics involved is very similar to that of the Sun, which is in turn well constrained by seismology. In particular, $M_V(\text{T-O})$ is quite insensitive to uncertainties related to model atmospheres or convection modeling (see also Freytag & Salaris 1999). Chaboyer et al suggested that no significant changes (more than $\sim 5\%$) in the derived ages of globular clusters are expected from future improvements in stellar models. Conversely, distance and abundance determinations are far from definite, and the quasi-verticalness of isochrones in the T-O region makes the determination of $M_V(\text{T-O})$ difficult (see Vandenberg et al 1996). Further revision of the ages is therefore not excluded. Also a global agreement between an entire globular cluster sequence and the corresponding model isochrone is far from being reached.

Age of the Universe. The ages of the oldest objects in the Galaxy, the most metal-poor halo or globular cluster stars, provide a minimum value for the age of the Universe T_U . Globular cluster ages (10-13 Gyr) from comparisons of isochrones with observed $M_V(\text{T-O})$ are presently the most reliable, but two independent methods look promising:

- Thorium (half-life 14.05 Gyr) has been detected and measured by Sneden et al (1996) in an ultra-metal-poor giant, too faint for observation by Hipparcos, and the star radioactive decay age is estimated to be 15 ± 4 Gyr. In the future, such observations of more stars and the possible detection of Rhenium and Uranium could provide strong constraints for T_U .
- Observations of (faint) white dwarfs (WD) in globular clusters are now within reach of experiments on board *HST*, and a lower limit to the age of WD in M4 of ~ 9 Gyr has been derived from a comparison with theoretical WD cooling curves (Richer et al 1997). Future access to cooler and fainter objects will better constrain T_U .

According to Sandage & Tammann (1997) and Saha et al (1999) the Hubble constant H_0 should be in the range $55 \pm 5 \text{ km.s}^{-1}.\text{Mpc}^{-1}$, which implies $T_U =$

$\frac{2}{3}H_0^{-1} \approx 11 - 13.5$ Gyr, indicating that no strong discrepancy with the age of the oldest known stars remains.

5.2 *Variable Stars*

I shall not discuss the revisions of the distance scale based on pulsating stars (RR Lyrae, Cepheids, Miras, high-amplitude δ Scuti stars) because this topic has been extensively reviewed by Caputo (1998) and Reid (1999).

Both new insight as well as new questions about the physics governing pulsating stars have been generated from the combination of Hipparcos distances with asteroseismic data. When the magnitude of a star is modified and its error box reduced, the mass and evolutionary stage attributed to the star may be modified. For variable stars, a different evolutionary stage may give a drastically different eigenmode spectrum, and in turn may change the mode identification and asteroseismic analysis (see Liu et al 1997). Høg & Petersen (1997) showed that for the two double-mode, high-amplitude δ Scuti variables SX Phe and AI Vel, the masses derived on one hand from stellar envelope models and pulsation theory, and on the other hand from the position in the H-R diagram through stellar evolution models are in nice agreement if the Hipparcos parallaxes (accurate to 5-6%) are used. Further implications of Hipparcos distances on the understanding of δ Scuti stars, λ Bootis, and rapidly oscillating Ap stars have been discussed in several papers (see for instance Audard et al 1998, Viskum et al 1998, Paunzen et al 1998, Matthews et al 1999), whereas the physical processes relevant to the Asymptotic Giant Branch and pulsation modeling of Miras and Long Period Variables were examined by Barthès (1998, see also references therein).

5.3 *White Dwarfs*

The white dwarf (WD) mass-radius (M-R) relation was first derived by Chandrasekhar (1931) from the theory of stars supported by the fully degenerate electron gas pressure. It has been refined by Hamada & Salpeter (1961), who calculated zero-temperature (fully degenerate) WD models of different chemical composition (He, C, Mg, Si, S, and Fe) and by Wood (1995), who calculated WD models with carbon cores and different configurations of hydrogen and/or helium layers and followed the thermal evolution of WD as they cool. Although theoretic-

cal support is strong, it has long been difficult to confirm the relation empirically because of (1) the very few available WD with measures of masses and radii, (2) the size of the error bars and (3) the intrinsic mass distribution of the WD, which concentrates them in only a small interval around $0.6 M_{\odot}$ (Schmidt 1996).

The M-R relation, assuming that WD have a carbon core, is a basic underlying assumption in most studies of WD properties. It serves to determine the mass of WD, and in turn their mass distribution and luminosity function. It is important because WD feature in many astrophysical applications such as the calibration of distances to globular clusters (Renzini et al 1996) or the estimate of the age of Galactic disk and halo by means of WD cooling sequences (see Winget et al 1987, d'Antona & Mazzitelli 1990). The more precisely the M-R relation is defined by observations, the better the tests of theoretical models of WD interiors that can be undertaken. These include tests of the inner chemical composition of WD, thickness of the hydrogen envelope of DA WD, or the characterization of their strong inner magnetic fields.

Depending on the white dwarf considered, the empirical M-R relation can be obtained by different means:

1. *Surface brightness method.* If T_{eff} and $\log g$ are determined (generally from spectroscopy), then model atmospheres allow calculation of the energy flux at the surface of the star, which when compared to the flux on Earth yields the angular diameter ϕ (see Schmidt 1996). The radius R is obtained from the parallax and ϕ , M is deduced from R and $\log g$. This method requires high-resolution spectra and largely depends on model atmospheres.
2. *Gravitational redshift.* The strong gravitational field at the surface of a WD causes a redshift of the spectral lines, the size of which depends on the gravitational velocity $v_{\text{grs}} = \frac{GM}{Rc}$ (c is the speed of light). If v_{grs} can be measured and the gravity is known, then M and R can easily be obtained independently of the parallax. v_{grs} can only be measured in WD members of binary systems, common proper motion pairs (CPM), or clusters because the radial velocity is required to distinguish the gravitational redshift from the line shift due to Doppler effect. Also, very high-resolution spectra are needed.
3. *WD in visual binary systems.* Masses may be derived directly from the

orbital parameters through the Kepler's third law, provided the parallax is known. Radii are derived from the knowledge of T_{eff} and distances.

More than 15 years ago, when the Hipparcos project began, uncertainties on WD ground-based parallaxes were at least 10 mas. During the last 10 years, due to great instrumental progress, parallax determinations were improved by a factor of about 2, and more accurate atmospheric parameters T_{eff} , g and v_{grs} were obtained. In the meantime, Hipparcos observed 22 white dwarfs (11 field WD, 4 WD in visual binaries, and 7 in CPM systems) among which 17 are of spectral type DA. Although they are close to the faint magnitude limit of Hipparcos, the mean accuracy on their parallaxes is $\sigma_{\pi} \simeq 3.6$ mas (Vauclair et al 1997).

Vauclair et al (1997) and Provencal et al (1998) studied the whole sample of WD observed by Hipparcos. The M-R relation is narrower and most points are within 1σ of Wood's (1995) evolutionary models of WD with carbon cores and hydrogen surface layers. The theoretical shape is still difficult to confirm because of the lack of objects in the regions of either high or low mass. Furthermore, the error bars are still too large to distinguish fine features of the theoretical models, such as between evolutionary and zero-temperature sequences or thick and thin hydrogen envelopes (Vauclair et al 1997), except for some particular stars (Shipman et al 1997, Provencal et al 1998). Other effects such as alterations due to strong internal magnetic fields are not yet testable (Suh & Mathews 2000).

WD in binary systems. Prior to Hipparcos, Sirius B was the only star roughly located on the expected theoretical M-R relations; the others (Procyon B, 40 Eridani B and Stein 2051) were at least 1.5σ below the theoretical position (see Figure 1 in Provencal et al 1998). After Hipparcos, as shown by Provencal et al, the error on the radius is dominated by errors on flux and T_{eff} . On the other hand, the parallax error still dominates the error on mass, except for Procyon where the error on the component separation plays a major role.

- Sirius B is more precisely located on a Wood's (1995) M-R relation for a DA white dwarf of the observed T_{eff} with a thick H layer and carbon core (Holberg et al 1998). Also compatible with Wood's thick H layer models is the position of V471 Tau, a member of an eclipsing binary system for which the Hipparcos parallax supports the view that it is a member of the Hyades (Werner & Rauch 1997, Barstow et al 1997). The mass of 40 Eri B

increased by 14%. The star is now back on Hamada & Salpeter's (1961) M-R relation for carbon cores, making it compatible with single star evolution (Figure 1 by Shipman et al 1997) and it does not appear to have a thick H layer. Sirius B (the most massive known WD) and 40 Eri B (one of the less massive) nicely anchor the high-mass and low-mass limits of the M-R relation.

- The case of Procyon B remains puzzling. The position is not compatible with models with carbon cores, and would be better accounted for with iron or iron-rich core models (Provencal et al 1997). Provencal et al (1998) also examined seven white dwarf members of CPM pairs (more distant and fainter than WD in visual binaries) with Hipparcos distances and gravitational redshift measurements. They showed that two of them also lie on theoretical M-R relations corresponding to iron cores. This is not predicted by current stellar evolution theory, and further work is required to clarify this problem.

In conclusion, better distances from Hipparcos and high-resolution spectroscopy has allowed better assessment of the theoretical M-R relation for white dwarfs, and has shown evidence for difficulties for a few objects that do not appear to have carbon cores. Future progress will come from further parallax improvements and from better T_{eff} , v_{grs} , magnitudes, and orbital parameters for visual binaries. A better understanding of the atmospheres is required: convection plays a role in the cooler WD, additional pressure effects due to undetectable helium affect the gravity determination, and incorrect H layer thickness estimates change the mass attributed to WD. Further information coming from asteroseismology or spectroscopy would help.

6 FUTURE INVESTIGATIONS

Hipparcos has greatly enlarged the available stellar samples with accurate and homogeneous astrometric and photometric data. To fully exploit this new information, many studies have been undertaken (several hundred papers devoted to stellar studies based on or mentioning Hipparcos data can be found in the literature), therefore the present review could not be fully exhaustive.

The Hipparcos mission succeeded in clarifying our knowledge of nearby objects,

and allowed first promising studies of rarer or farther objects. After Hipparcos, the theory of stellar structure and evolution is further anchored, and some of its physical aspects have been better characterized. For instance, new indications that the evolution of low-mass stars is significantly modified by microscopic diffusion have been provided by fine studies of the H-R diagram, and consequences for age estimates or surface abundance alterations have been further investigated. On the other hand, Hipparcos left us with intriguing results that raised new questions. For example, the unexpected position of the white dwarf Procyon B on a theoretical mass-radius relation corresponding to iron cores is still not understood.

Today, uncertainties on distances of nearby stars have been reduced significantly such that other error sources emerge to dominate, hindering further progress in the fine characterization of stellar structure. Progress on atmosphere modeling is worth being pursued, for it has implications for observational parameters (effective temperatures, gravities, abundances, bolometric corrections), theoretical models (outer boundary conditions), and color calibrations. A thorough theoretical description of transport processes (convection, diffusion) and related effects (rotation, magnetic fields) is needed to improve stellar models, as well as further improvements or refinements in microscopic physics (low-temperature opacities, nuclear reaction rates in advanced evolutionary stages).

What is now needed from the observational side is (1) enlarged samples of rare objects (distant objects, faint objects or objects undergoing rapid evolutionary phases), (2) an increased number of more “common” objects with extremely accurate data (including masses), and (3) a census over all stellar populations.

These goals should be (at least partially) achieved by future astrometric missions. The NASA Space Interferometry Mission (SIM), scheduled for launch in 2006, will have the capability to measure parallaxes to $4 \mu\text{arcsecond}$ and proper motions to $1\text{-}2 \mu\text{arcsecond}$ per year down to the 20th magnitude which represents a gain of three orders of magnitude with respect to Hipparcos (Peterson & Shao 1997). The ESA candidate mission GAIA is dedicated to the observation of about one billion objects down to $V \simeq 20$ mag (and typical $\sigma_\pi \sim 10 \mu\text{arcsecond}$ at $V=15$ mag). GAIA will also provide multi-color, multi-epoch photometry for each object, and will give access to stars of various distant regions of the Galaxy (halo, bulge, thin and thick disk, spiral arms). It is aimed to be launched in 2009

(Perryman et al 1997b).

Asteroseismology has already proved to be a unique tool to probe stellar interiors. Space experiments are under study. The first step will be the COROT mission (aimed to be launched in 2003), designed to detect and characterize oscillation modes in a few hundred stars, including solar-type stars and δ Scuti stars (see Baglin 1998).

7 Acknowledgments

I enjoyed very much working with Ana Gómez, Roger and Giusa Cayrel, João Fernandes, Michael Perryman, Noël Robichon, Annie Baglin, Jean-Claude Mermilliod, Marie-Noël Perrin, Frédéric Arenou, Catherine Turon, and Corinne Charbonnel on the various subjects presented here. I particularly thank Roger Cayrel, Annie Baglin, Michael Perryman, and Catherine Turon for a careful reading of the original manuscript. I am also very grateful to Allan Sandage for his remarks and suggestions which helped improving the paper. I am especially grateful to Frédéric Thévenin, Hans-Günter Ludwig, Misha Haywood, Don Vandenberg, Marie-Jo Goupil, Pierre Morel, Jordi Carme and Franck Thibault for fruitful discussions and advice. The University of Rennes 1 is acknowledged for working facilities. This review has made use of NASA's Astrophysics Data System Abstract Service mirrored at CDS (Centre des Données Stellaires, Strasbourg, France).

Literature Cited

1. Abbett WP, Beaver M, Davids B, Georgobiani D, Rathbun P, Stein RF. 1997. *Ap. J.* 480:395-99
2. Alexander DR, Ferguson JW. 1994. *Ap. J.* 437:879-91
3. Allard F, Hauschildt PH, Alexander DR, Starrfield S. 1997. *Annu. Rev. Astron. Astrophys.* 35:137-77
4. Alonso A, Arribas S, Martínez-Roger C. 1995. *Astron. Astrophys.* 297:197-215
5. Alonso A, Arribas S, Martínez-Roger C. 1996a. *Astron. Astrophys. Suppl. Ser.* 117:227-54
6. Alonso A, Arribas S, Martínez-Roger C. 1996b. *Astron. Astrophys.* 313:873-90
7. Andersen J. 1991. *Astron. Astrophys. Rev.* 3:91-126
8. Antonello E, Pasinetti Fracassini LE. 1998. *Astron. Astrophys.* 331:995-1001
9. Arenou F, Lindegren L, Froeschlé M, Gómez AE, Turon C et al. 1995. *Astron. Astrophys.* 304:52-60

10. Axer M, Fuhrmann K, Gehren T. 1994. *Astron. Astrophys.* 291:895-909
11. Axer M, Fuhrmann K, Gehren T. 1995. *Astron. Astrophys.* 300:751-68
12. Audard N, Kupka F, Morel P, Provost J, Weiss WW. 1998. *Astron. Astrophys.* 335:954-58
13. Baglin A. 1999. *Highlights of Astronomy*, ed. J Andersen, XXIII rd IAU General Assembly, 11B:555, Dordrecht: Kluwer
14. Baglin A and the COROT team 1998. In *New Eyes to See Inside the Sun and the Stars*, ed. F-L Deubner, J Christensen-Dalsgaard, D Kurtz, *IAU Symp 185*, p. 301. Dordrecht: Kluwer
15. Balbes MJ, Boyd RN, Mathews GJ. 1993. *Ap. J.* 418:229-34
16. Barnes TG, Evans DS, Moffett TJ. 1978. *MNRAS* 183:285-304
17. Barstow MA, Holberg JB, Cruise AM, Penny AJ. 1997. *MNRAS* 290:505-14
18. Barthès D. 1998. *Astron. Astrophys.* 333:647-57
19. Battrick B, ed. 1997. *HIPPARCOS Venice '97: Presentation of the Hipparcos and Tycho Catalogues and First Astrophysical Results of the Hipparcos Space Astrometry Mission*. Sci. Coord. MAC Perryman, PL Bernacca, ESA SP-402. Noordwijk, The Netherlands: ESA Publ. Div. ESTEC
20. Belikov AN, Hirte S, Meusinger H, Piskunov E, Schilbach E. 1998. *Astron. Astrophys.* 332:575-85
21. Benedict GF, McArthur BJ, Nelan E, Story D, Whipple AL et al. 1994. *PASP* 106:327-36
22. Bernkopf J. 1998. *Astron. Astrophys.* 332:127-34
23. Bessell MS, Castelli F, Plez B. 1998. *Astron. Astrophys.* 333:231-50
24. Blackwell DE, Lynas-Gray AE. 1998. *Astron. Astrophys. Suppl. Ser.* 129:505-15
25. Blackwell DE, Petford AD, Arribas S, Haddock DJ, Selby MJ. 1990. *Astron. Astrophys.* 232:396-410
26. Boesgaard AM, Friel ED. 1990. *Ap. J.* 351:467-91
27. Böhm-Vitense E. 1958. *Zeitschrift f. Astrophysik* 45:108-43
28. Bressan AG, Bertelli G, Chiosi C. 1981 *Astron. Astrophys.* 102:25-30
29. Brett JM. 1995. *Astron. Astrophys.* 295:736-54
30. Brown AGA, Arenou F, van Leeuwen F, Lindegren L, Luri X. 1997. See Battrick 1997, pp. 63-68
31. Brown TM, Christensen-Dalsgaard J, Weibel-Mihalas B, Gilliland RL. 1994. *Ap. J.* 427:1013-34
32. Caputo F. 1998. *Astron. Astrophys. Rev.* 9:33-61
33. Carbon FC. 1979. *Annu. Rev. Astron. Astrophys.* 17:513-49
34. Castellani V, Ciacio F, Degl'Innocenti S, Fiorentini G. 1997. *Astron. Astrophys.* 322:801-6
35. Cayrel R, Castelli F, Katz D, van't Veer C, Gómez AE, Perrin M-N. 1997a. See Battrick 1997, pp. 433-35
36. Cayrel R, Faurobert-Scholl M, Feautrier N, Spielfieldel A, Thvenin F. 1996. *Astron. Astrophys.* 312:549-52
37. Cayrel R, Lebreton Y, Perrin M-N, Turon C. 1997b. See Battrick 1997, pp. 219-24

38. Cayrel de Strobel G, Crifo F, Lebreton Y. 1997a See Battrick 1997, pp. 687-88
39. Cayrel de Strobel G, Soubiran C, Friel ED, Ralite N, Franois P. 1997b. *Astron. Astrophys. Suppl. Ser.* 124:299-305
40. Chaboyer B. 1998. In *Post-Hipparcos Cosmic Candles*, ed. A Heck, F Caputo, *Astrophys. Space Sci. Libr.* 237:111-25, Dordrecht: Kluwer
41. Chaboyer B, Demarque P, Kernan PJ, Krauss LM. 1998. *Ap. J.* 494:96-110
42. Chabrier G, Baraffe I. 1997. *Astron. Astrophys.* 327:1039-53
43. Chandrasekhar S. 1931. *MNRAS* 91:456
44. Chieffi A, Straniero O, Salaris M. 1995. *Ap. J.* 445:L39-42
45. Christensen-Dalsgaard J. 1982. *MNRAS* 199:735-61
46. Christensen-Dalsgaard J, Dppen W. 1992. *Astron. Astrophys. Rev.* 4:267-361
47. Christensen-Dalsgaard J, Proffitt CR, Thompson MJ. 1993. *Ap. J.* 403:L75-78
48. Clementini G, Gratton RG, Carretta E, Sneden C. 1999. *MNRAS* 302:22-36
49. Code AD, Davis J, Bless RC, Hanbury Brown R. 1976. *Ap. J.* 203:417-34
50. D'Antona F, Mazzitelli I. 1990. *Annu. Rev. Astron. Astrophys.* 28:139-81
51. Di Benedetto GP. 1998. *Astron. Astrophys.* 339:858-71
52. Dravins D, Lindegren L, Madsen S, Holmberg J. 1997. See Battrick 1997, pp. 733-38
53. Edmonds P, Cram L, Demarque P, Guenther DB, Pinsonneault MH. 1992. *Ap. J.* 394:313-19
54. Eggen OJ, Sandage A. 1962. *Ap. J.* 136:735-47
55. Eur. Space Agency. 1997. *The Hipparcos and Tycho Catalogues*, Eur. Space Agency Spec. Publ. 1200. Noordwijk, The Netherlands: ESA Publ. Div. ESTEC
56. Fernandes J, Lebreton Y, Baglin A 1996. *Astron. Astrophys.* 311:127-34
57. Fernandes J, Lebreton Y, Baglin A, Morel P. 1998. *Astron. Astrophys.* 338:455-64
58. Fernandes J, Neuforge C. 1995. *Astron. Astrophys.* 295:678-84
59. Freytag B, Ludwig HG, Steffen M. 1999. In: "Theory and Tests of Convection in Stellar Structure", ASP, Conference Series, Vol. 173, eds: A. Gime'nez, E.F. Guinan, and B. Montesinos, pp. 225-28
60. Freytag B, Salaris M. 1999. *Ap. J.* 513:L49-52
61. Fuhrmann K. 1998. *Astron. Astrophys.* 330:626-30
62. Fuhrmann K, Pfeiffer M, Frank C, Reetz J, Gehren T. 1997. *Astron. Astrophys.* 323:909-22
63. Gatewood G, Kiewiet de Jonge J, Persinger T. 1998. *Astron. J.* 116:1501-03
64. Goupil M-J, Dziembowski WA, Goode PR, Michel E. 1996. *Astron. Astrophys.* 305:487-97
65. Gratton RG, Fusi Pecci F, Carretta E, Clementini G, Corsi CE, Lattanzi M. 1997. *Ap. J.* 491:749-71
66. Grevesse N, Sauval AJ. 1999. *Astron. Astrophys.* 347:348-54
67. Groenewegen MAT, Salaris M . 1999. *Astron. Astrophys.* 348:L33-36
68. Gustafsson B. 1998. In *Fundamental Stellar Properties: The Interaction between Observation and Theory*, ed. TR Bedding, AJ Booth, J Davis, *IAU Symp 189*, p. 261, Dordrecht: Kluwer

69. Gustafsson B, Bell RA, Eriksson K, Nordlund Å. 1975 *Astron. Astrophys.* 42:407-32
70. Hamada T, Salpeter EE. 1961. *Ap. J.* 134:683-98
71. Hanson RB. 1979. *MNRAS* 186:875-96
72. Harris HC, Dahn CC, Monet DG. 1997. See Battrick 1997, pp. 105-11
73. Harrison TE, McNamara BJ, Szkody P, McArthur BE, Benedict GF et al. 1999. *Ap. J.* 515:L93-96
74. Henyey LG, Wilets L, Böhm KH, LeLevier R, Levee RD. 1959. *Ap. J.* 129:628-36
75. Høg E, Petersen JO. 1997. *Astron. Astrophys.* 323:827-30
76. Holberg JB, Barstow MA, Bruhweiler FC, Cruise AM, Penny AJ. 1998. *Ap. J.* 497:935-42
77. Huebner WF, Merts AL, Magee NH, Argo MF. 1977. *Los Alamos Sci. Rep. LA-6760-M*
78. Iglesias CA, Rogers FJ. 1996. *Ap. J.* 464:943-53
79. Izotov YI, Thuan TX, Lipovetsky VA. 1997. *Ap. J. Suppl.* 108:1-39
80. Jimenez R, Flynn C, Kotoneva E. 1998. *MNRAS* 299:515-19
81. King JR, Stephens A, Boesgaard AM, Deliyannis CP. 1998. *Astron. J.* 115:666-84
82. Kosovichev AG, Christensen-Dalsgaard J, Däppen W, Dziembowski WA, Gough DO, Thompson MJ. 1992. *MNRAS* 259:536-58
83. Kovalevsky J. 1998. *Annu. Rev. Astron. Astrophys.* 36:99-129
84. Kurucz RL. 1979. *Ap. J. Suppl.* 40:1-340
85. Kurucz RL. 1991. In *Stellar Atmospheres: Beyond Classical Models*, ed. L Crivellari, I Hubeny, DG Hummer, *NATO ASI Ser.*, pp. 441-48, , Dordrecht: Kluwer
86. Kurucz RL. 1993. In *Peculiar versus Normal Phenomena in A-type and Related Stars*, ed. MM Dworetzky, F Castelli, R Faraggiana, *IAU Colloq. 138*, pp. 87, San Francisco: Astron. Soc. Pac.
87. Layden AC. 1998. In *Post-Hipparcos Cosmic Candles*, ed. A Heck, F Caputo, *Astrophys. Space Sci. Lib.* 237:37-52, Dordrecht: Kluwer
88. Lebreton Y. 2000. See Livio, 2000, pp. 107
89. Lebreton Y, Gómez AE, Mermilliod J-C, Perryman MAC. 1997a. See Battrick 1997, pp. 231-36
90. Lebreton Y, Michel E, Goupil MJ, Baglin A, Fernandes J. 1995. In *Astronomical and Astrophysical Objectives of Sub-Milliarcsecond Optical Astrometry*, ed. E Høg, PK Seidelman, *IAU Symp 166*, pp. 135-42, Dordrecht: Kluwer
91. Lebreton Y, Perrin M-N, Cayrel R, Baglin A, Fernandes J. 1999. *Astron. Astrophys.* 350:587-97
92. Lebreton Y, Perrin M-N, Fernandes J, Cayrel R, Baglin A, Cayrel de Strobel G. 1997b. See Battrick 1997, pp. 379-82
93. Lindegren L. 1995. *Astron. Astrophys.* 304:61-68
94. Lindegren L, Mignard F, Sderhjelm S, Badiali M, Bernstein HH et al. 1997. *Astron. Astrophys.* 323:L53-56
95. Liu YY, Baglin A, Auvergne M, Goupil M-J, Michel E. 1997. See Battrick 1997, pp. 363-66
96. Livio M. ed. 2000. *Unsolved Problems in Stellar Evolution* STScI May 1998 Symp., Cam-

- bridge: Cambridge University Press
97. Ludwig HG, Freytag B, Steffen M. 1999. *Astron. Astrophys.* 346:111-24
 98. Lutz TE, Kelker DH. 1973. *PASP* 85:573-78
 99. Lydon TJ, Fox PA, Sofia S. 1993. *Ap. J.* 413:390-400
 100. Maeder A, Mermilliod J-C. 1981. *Astron. Astrophys.* 93:136-49
 101. Maeder A, Peytremann E. 1972. *Astron. Astrophys.* 21:279-84
 102. Martin C, Mignard F. 1998. *Astron. Astrophys.* 330:585-99
 103. Martin C, Mignard F., Froeschl M. 1997. *Astron. Astrophys. Suppl. Ser.* 122:571-80
 104. Martin C, Mignard F, Hartkopf WI, McAlister HA. 1998. *Astron. Astrophys. Suppl. Ser.* 133:149-62
 105. Matthews JM, Kurtz DW, Martinez P. 1999. *Ap. J.* 511:422-28
 106. Mc Williams A. 1997. *Annu. Rev. Astron. Astrophys.* 35:503-56
 107. Mermilliod J-C. 2000. In *Very Low-Mass Stars and Brown Dwarfs in Stellar Clusters and Associations*, eds R Rebolo, MR Zapatorio-Osorio, Cambridge: Cambridge University Press
 108. Mermilliod J-C, Turon C, Robichon N, Arenou F, Lebreton Y. 1997. See Battrick 1997, pp. 643-50
 109. Michel E, Hernández MM, Houdek G, Goupil M-J, Lebreton Y et al. 1999. *Astron. Astrophys.* 342:153-66
 110. Mignard F. 1997. See Battrick 1997, pp. 5-10
 111. Mihalas D, Däppen W, Hummer DG. 1988. *Ap. J.* 331:815-25
 112. Morel P, Baglin A. 1999. *Astron. Astrophys.* 345:156-62
 113. Morel P, Morel Ch, Provost J, Berthomieu G. 2000. *Astron. Astrophys.* 354:636-44
 114. Morel P, van 't Veer C, Provost J, Berthomieu G, Castelli F et al. 1994 *Astron. Astrophys.* 286:91-102
 115. Narayanan VK, Gould A. 1999a. *Ap. J.* 515:256-64
 116. Narayanan VK, Gould A. 1999b. *Ap. J.* 523:328-39
 117. Ng YK, Bertelli G. 1998. *Astron. Astrophys.* 329:943-50.
 118. Nissen PE. 1976. *Astron. Astrophys.* 50:343-52
 119. Nissen PE. 1998. In *The First MONS Workshop: Science with a Small Space Telescope*, eds. H Kjeldsen, TR Bedding, pp 99-104, Aarhus: Aarhus Universitet
 120. Nissen PE, Høg E, Schuster WJ. 1997. See Battrick 1997, pp. 225-30
 121. Noels A, Fraipont D, Gabriel M, Grevesse N, Demarque P eds. 1995. *Stellar Evolution: What Should Be Done?* Proc. 32nd Liège International Astrophysical Coll., Liège: Univ. de Liège
 122. Noels A, Grevesse N, Magain P, Neuforge C, Baglin A, Lebreton Y. 1991. *Astron. Astrophys.* 247:91-94
 123. Pagel BEJ, Portinari L. 1998. *MNRAS* 298:747-52
 124. Paunzen E, Weiss WW, Kuschnig R, Handler G, Strassmeier KG et al. 1998. *Astron. Astrophys.* 335:533-38

125. Pérez-Hernández F, Claret A, Hernández MM, Michel E. 1999. *Astron. Astrophys.* 346:586-98
126. Perryman MAC, Brown AGA, Lebreton Y, Gmez AE, Turon C et al. 1998. *Astron. Astrophys.* 331:81-120
127. Perryman MAC, Lindegren L, Kovalevsky J, Høg E, Bastian U et al. 1997a. *Astron. Astrophys.* 323:L49-L52
128. Perryman MAC, Lindegren L, Turon C. 1997b. See Battrick 1997, pp. 743-48
129. Peterson DM, Shao M. 1997. See Battrick 1997, pp. 749-53
130. Peterson DM, Solensky R. 1988. *Ap. J.* 333:256-66
131. Pinsonneault MH. 1997. *Annu. Rev. Astron. Astrophys.* 35:557-605
132. Pinsonneault MH, Stauffer J, Soderblom DR, King JR, Hanson RB. 1998. *Ap. J.* 504, 170-91
133. Platais I, Kozhurina-Platais V, van Leeuwen F. 1998. *Astron. J.* 116:2423-30
134. Pont F, Mayor M, Turon C, VandenBerg DA. 1998. *Astron. Astrophys.* 329: 87-100
135. Pont F, Charbonnel C, Lebreton Y, Mayor M, Turon C, VandenBerg DA. 1997. See Battrick 1997, pp. 699-704
136. Popper DM. 1998. *PASP* 110:919-22
137. Pourbaix D, Neuforge-Verheecke C, Noels A. 1999. *Astron. Astrophys.* 344:172-76
138. Proffitt CR, VandenBerg DA. 1991. *ApJS* 77:473-514
139. Provencal JL, Shipman HL, Høg E, Thejll P. 1998. *Ap. J.* 494:759-67
140. Provencal JL, Shipman HL, Wesemael F, Bergeron P, Bond HE et al. 1997. *Ap. J.* 480:777-83
141. Reid IN. 1997. *Astron. J.* 114:161-79
142. Reid IN. 1998. *Astron. J.* 115:204-28
143. Reid IN. 1999. *Annu. Rev. Astron. Astrophys.* 37:191-237
144. Renzini A, Bragaglia A, Ferraro FR, Gilmozzi R, Ortolani S et al. 1996. *Ap. J.* 465:L23-26
145. Ribas I. 1999. PhD thesis. Univ. de Barcelona, Spain
146. Ribas I, Giménez A, Torra J, Jordi C, Oblak E. 1998. *Astron. Astrophys.* 330:600-4
147. Richard O, Vauclair S, Charbonnel C, Dziembowski WA. 1996. *Astron. Astrophys.* 312 1000-11
148. Richer HB, Fahlman GG, Ibata RA, Pryor C, Bell RA et al. 1997. *Ap. J.* 484:741-60
149. Robichon N, Arenou F, Turon C, Mermilliod J-C, Lebreton Y. 1997. See Battrick 1997, pp. 567-70
150. Robichon N, Arenou F, Lebreton Y, Turon C, Mermilliod J-C. 1999b. In *Harmonizing Cosmic Distance Scales in a Post-Hipparcos Era*, ed. D Egret, A Heck. ASP Conf. Ser. 167, p. 72-77
151. Robichon N, Arenou F, Mermilliod J-C, Turon C. 1999a. *Astron. Astrophys.* 345:471-84
152. Rogers FJ, Iglesias CA. 1992 *Ap. J. Suppl.* 79:507-68
153. Rogers FJ, Swenson FJ, Iglesias CA. 1996 *Ap. J.* 456:902-8
154. Roxburgh IW. 1997. In *Solar Convection and Oscillations and their Relationship*, SCORE

- '96, ed. FP Pijpers, J Christensen-Dalsgaard, C Rosenthal, *Astrophys. Space Sci. Lib.* 225:23-50, Dordrecht: Kluwer
155. Saha A, Sandage A, Labhardt L, Tammann GA, Macchetto FD, Panagia N. 1999. *Ap. J.* 486:1-20
156. Salaris M, Groenewen MAT, Weiss A. 2000. *Astron. Astrophys.* 355:299-307
157. Sandage A. 1970. *Ap. J.* 162:841-70
158. Sandage A. 1983. *Astron. J.* 88:1569-78
159. Sandage A, Tammann GA. 1997. In *Critical Dialogues in Cosmology*, ed. N Turok, pp. 130, Singapore: World Scientific
160. Saumon D, Chabrier G. 1991 *Phys. Rev. A* 44:5122-41
161. Schmidt H. 1996. *Astron. Astrophys.* 311:852-57
162. Schröder K-P. 1998. *Astron. Astrophys.* 334:901-10
163. Schwarzschild M. 1958. *Structure and Evolution of the Stars*. Princeton: Princeton University Press
164. Seaton MJ, Yan Y, Mihalas D, Pradhan AK. 1994. *MNRAS* 266:805-28
165. Shipman HL, Provencal JL, Høg E, Thejll P. 1997. *Ap. J.* 488:L43-46
166. Smith H. 1987. *Astron. Astrophys.* 188:233-38
167. Sneden C, McWilliam A, Preston GW, Cowan JJ, Burris DL, Armosky BJ. 1996. *Ap. J.* 467:819-40
168. Soderblom DR, King JR, Hanson RB, Jones BF, Fischer D et al. 1998. *Ap. J.* 504:192-99
169. Sderhjelm S. 1999. *Astron. Astrophys.* 341:121-40
170. Stein RF, Nordlund Å. 1998. *Ap. J.* 499:914-33
171. Suh I-S, Mathews GJ. 2000. *Ap. J.* 530:949-54
172. Talon S, Zahn J-P, Maeder A, Meynet G. 1997. *Astron. Astrophys.* 322:209-17
173. Thévenin F, Idiart TP. 1999. *Ap. J.* 521:753-63
174. Torres G, Stefanik RP, Latham DW. 1997a. *Ap. J.* 474:256-71
175. Torres G, Stefanik RP, Latham DW. 1997b. *Ap. J.* 479:268-78
176. Torres G, Stefanik RP, Latham DW. 1997c. *Ap. J.* 485:167-81
177. van Altena WF, Lee JT, Hoffleit ED. 1997b. *Baltic Astron* 6:27
178. van Altena WF, Lu C-L, Lee JT, Girard TM, Guo X et al. 1997a. *Ap. J.* 486:L123-27
179. VandenBerg DA, Bolte M, Stetson PB. 1996. *Annu. Rev. Astron. Astrophys.* 34:461-510
180. van Leeuwen F. 1997. *Space Science Reviews* 81:201-409
181. van Leeuwen F. 1999a. In *Harmonizing Cosmic Distance Scales in a Post-Hipparcos Era*, ed. D Egret, A Heck, ASP Conf. Ser. 167, p. 52-71
182. van Leeuwen F. 1999b. *Astron. Astrophys.* 341:L71-74
183. van Leeuwen F, Evans DW. 1998. *Astron. Astrophys. Suppl. Ser.* 130:157-172
184. van Leeuwen F, Evans DW, Grenon M, Grossmann V, Mignard F, Perryman MAC. 1997. *Astron. Astrophys.* 323:L61-64
185. Vauclair G, Schmidt H, Koester D, Allard N. 1997. *Astron. Astrophys.* 325:1055-62
186. Viskum M, Kjeldsen H, Bedding TR, Dall TH, Baldry IK et al. 1998. *Astron. Astro-*

phys. 335:549-60

187. Werner K, Rauch T. 1997. *Astron. Astrophys.* 324:L25-28
188. Wheeler JC, Sneden C, Truran JW. 1989. *Annu. Rev. Astron. Astrophys.* 27:279-349
189. Winget DE, Hansen CJ, Liebert J, Van Horn HM, Fontaine G et al. 1987. *Ap. J.* 315:L77-81
190. Wood MA. 1995, In *Proc. 9th European Workshop on White Dwarfs*, ed. D Koester, K Werner, pp. 41-45, Berlin: Springer-Verlag
191. Zahn J-P. 1992. *Astron. Astrophys.* 265:115-32

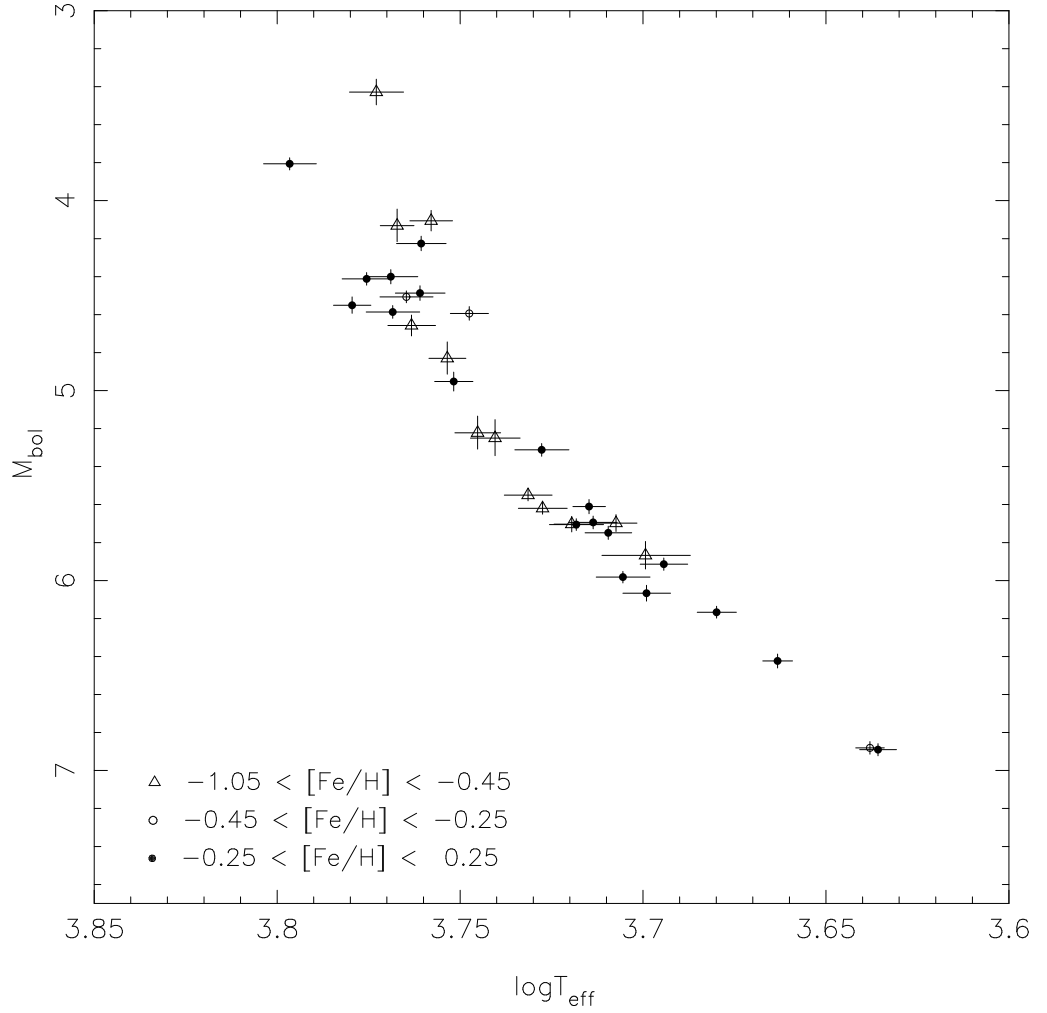


Figure 1: Hipparcos H-R diagram of the 34 best-known nearby stars. The parallax accuracies σ_{π}/π are in the range 0.003-0.041. Bolometric fluxes and effective temperatures are available from Alonso et al's (1995, 1996a) works ($\frac{\sigma_{F_{\text{bol}}}}{F_{\text{bol}}} \sim 2\%$ and $\frac{\sigma_{T_{\text{eff}}}}{T_{\text{eff}}} \sim 1.5\%$, see Section 2.2). Resulting $\sigma_{M_{\text{bol}}}$ are in the range 0.031-0.095 mag (from Lebreton et al 1999).

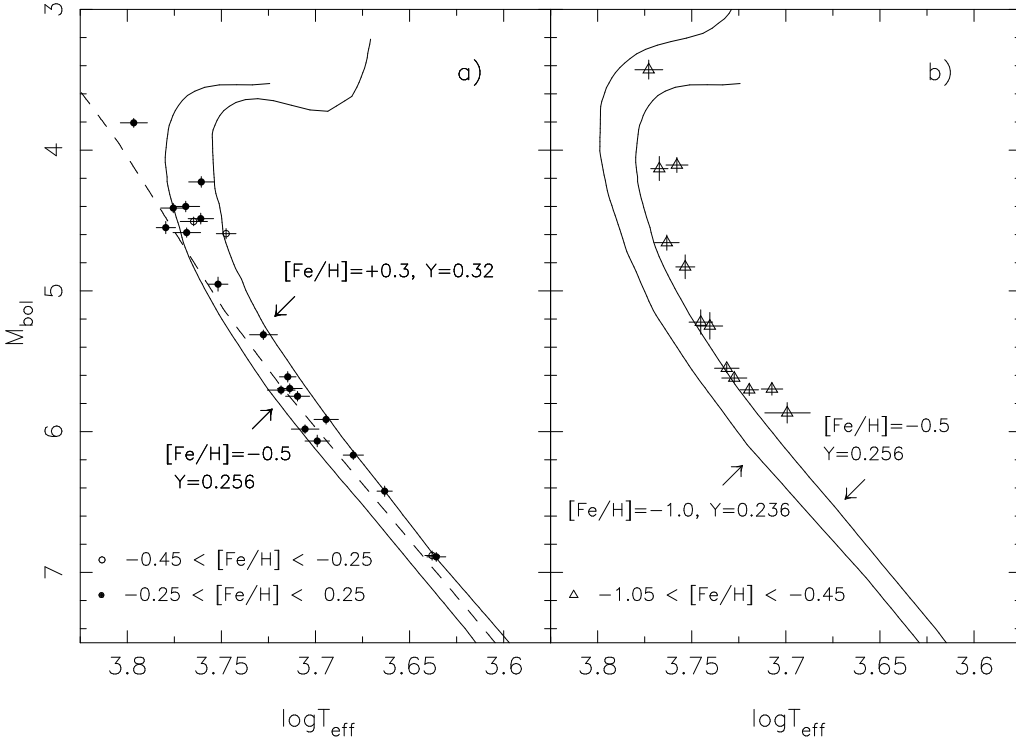


Figure 2: The sample of Figure 1 split into two metallicity domains. Figure 2a shows stars with $[\text{Fe}/\text{H}]$ close to solar ($[\text{Fe}/\text{H}] \in [-0.45, +0.25]$). Figure 2b shows moderately metal-deficient stars ($[\text{Fe}/\text{H}] \in [-1.05, -0.45]$). Theoretical isochrones are overlaid on the observational data. Figure 2a: the lower isochrone (10 Gyr) is for $[\text{Fe}/\text{H}] = -0.5$, $Y = 0.256$ and $[\alpha/\text{Fe}] = 0.4$; the upper isochrone (8 Gyr) is for $[\text{Fe}/\text{H}] = +0.3$, $Y = 0.32$ and $[\alpha/\text{Fe}] = 0.0$; the dashed line is a solar ZAMS ($\alpha_{\text{MLT}} = 1.65$, $Y_{\odot} = 0.266$ and $Z_{\odot} = 0.0175$). The brightest star is the young star γ Lep. Figure 2b: 2 isochrones (10 Gyr) with $[\alpha/\text{Fe}] = 0.4$, the lower is for $[\text{Fe}/\text{H}] = -1.0$, $Y = 0.236$ and the upper for $[\text{Fe}/\text{H}] = -0.5$, $Y = 0.256$. All stars but one are sitting above the region defined by the isochrones. $(\Delta Y/\Delta Z)_{\odot} = 2.2$ is obtained with Balbes et al's (1993) primordial helium $Y_{\text{p}} = 0.227$ (from Lebreton et al 1999).

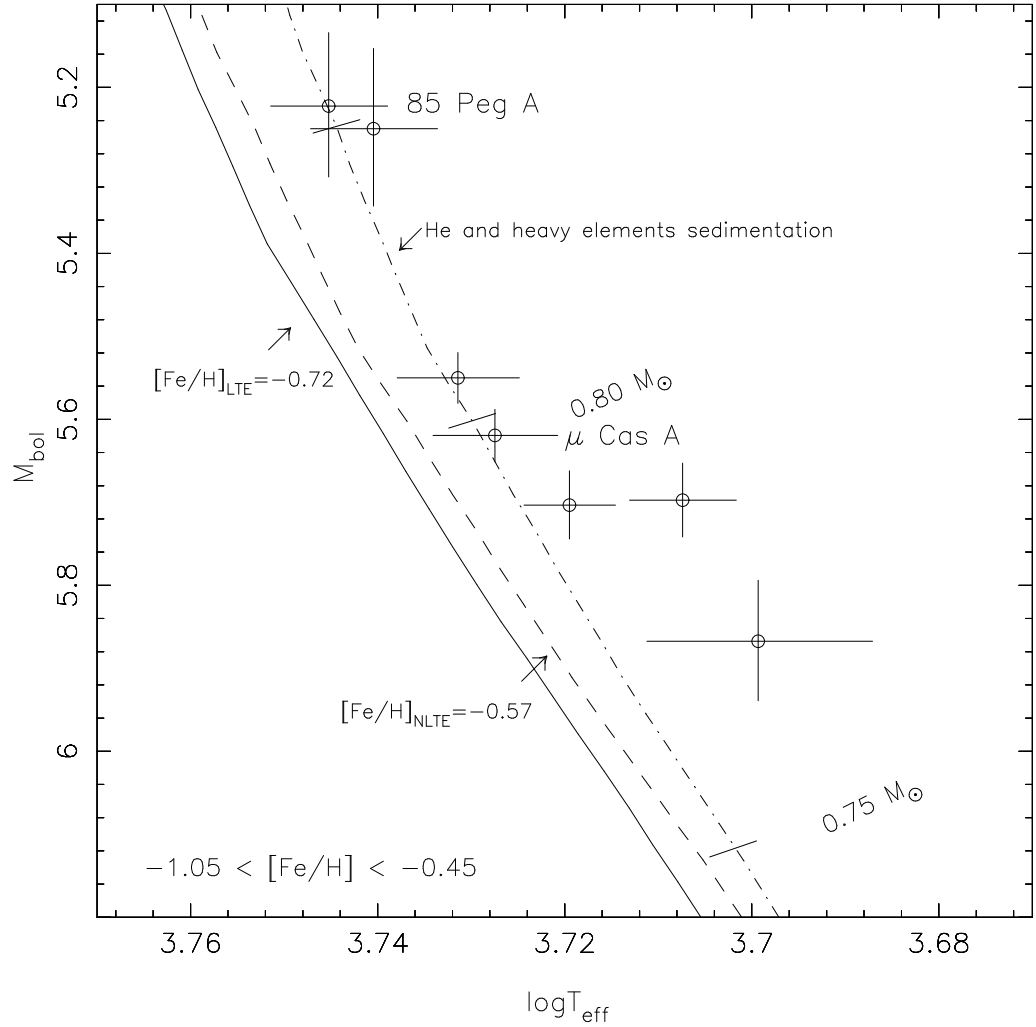


Figure 3: H-R diagram for the unevolved moderately metal deficient stars of Figure 2 (mean LTE metallicity $[\text{Fe}/\text{H}]_{\text{LTE}} = -0.72$, mean non-LTE value $[\text{Fe}/\text{H}]_{\text{NLTE}} = -0.57$, see text). Full and dashed lines are standard isochrones (10 Gyr) computed with, respectively, the $[\text{Fe}/\text{H}]_{\text{LTE}}$ and $[\text{Fe}/\text{H}]_{\text{NLTE}}$ values. The dot-dashed isochrone (10 Gyr) includes He and heavy elements sedimentation: at the surface it has $[\text{Fe}/\text{H}]_{\text{NLTE}} = -0.57$ but the initial $[\text{Fe}/\text{H}]$ was ≈ -0.5 . (from Lebreton et al 1999).

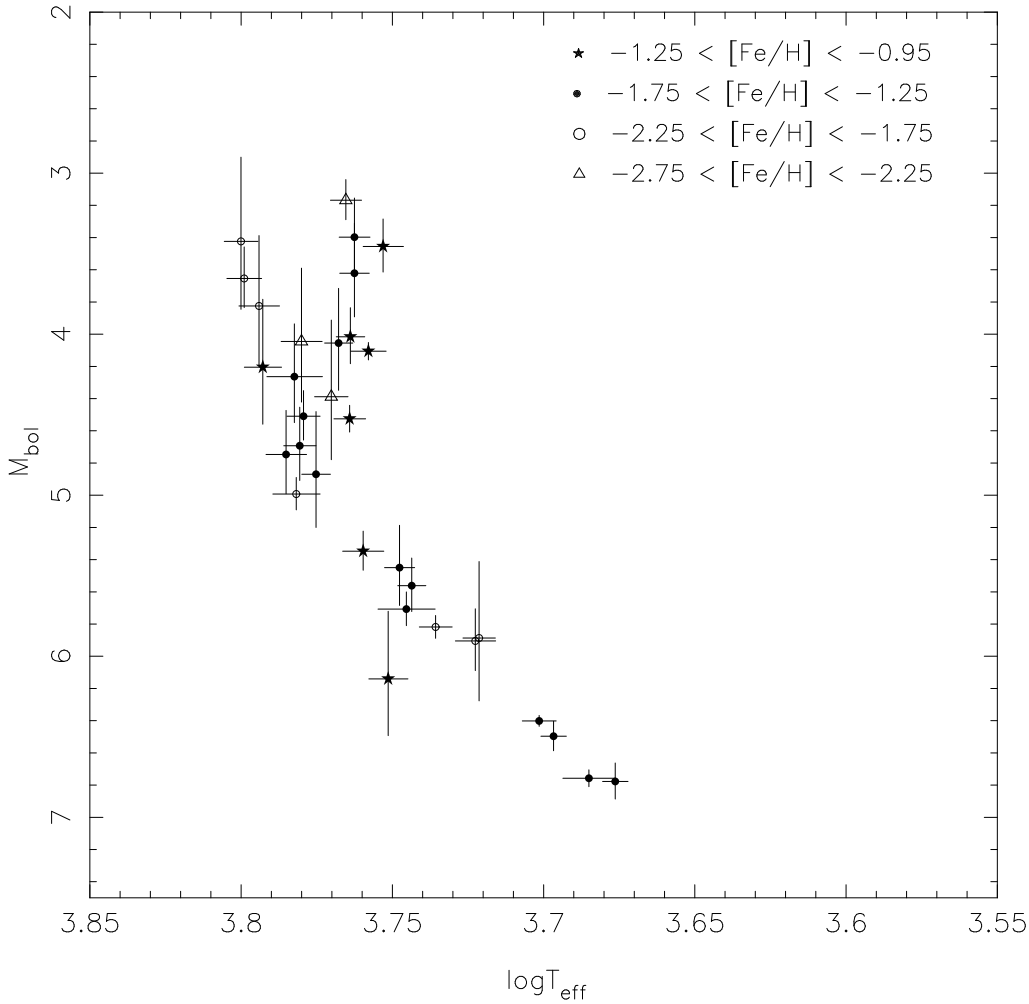


Figure 4: Hipparcos H-R diagram of the 32 halo stars with $\sigma_{\pi}/\pi < 0.22$ (the parallax accuracies σ_{π}/π are in the range 0.007-0.214). Bolometric fluxes and effective temperatures are available from Alonso et al's (1995, 1996a) works (see the caption for Figure 1). Resulting $\sigma_{M_{\text{bol}}}$ are in the range 0.03-0.48 mag. A bunch of subgiants emerges with an isochrone-like shape (from Cayrel et al 1997b).

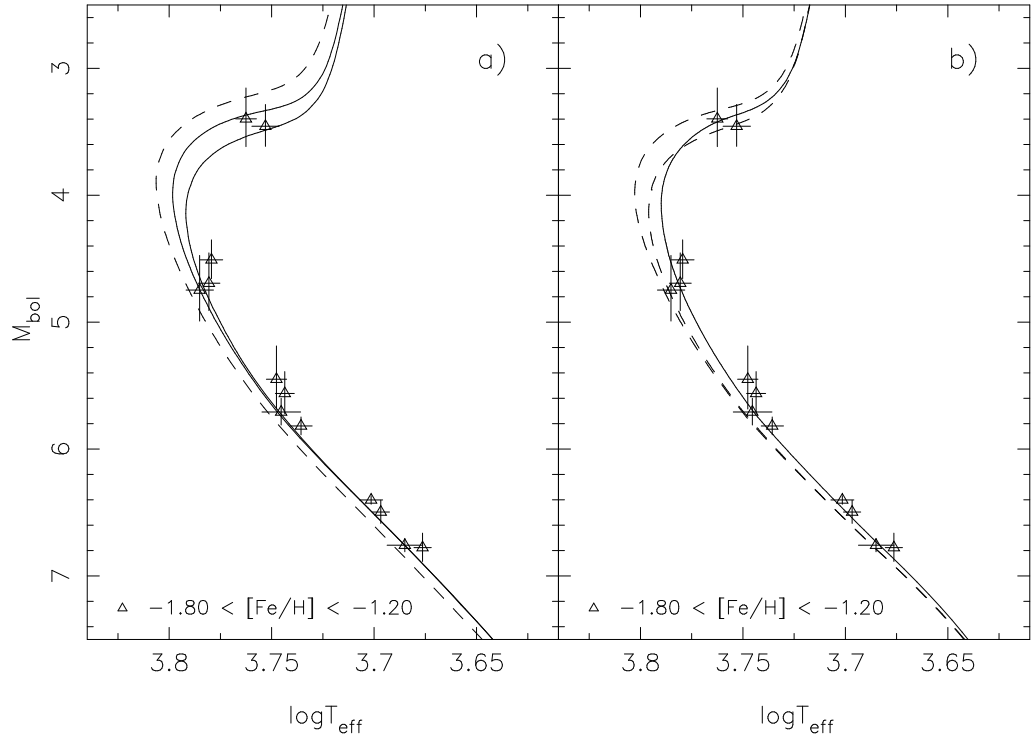


Figure 5: Hipparcos H-R diagram of 13 halo stars with $[\text{Fe}/\text{H}]_{\text{LTE}} = -1.5 \pm 0.3$ and $\sigma_{\pi}/\pi < 0.12$ (the parallax accuracies σ_{π}/π are in the range 0.01-0.12). Bolometric fluxes and effective temperatures are available from Alonso et al's (1995, 1996a) works (see the caption for Figure 1). Resulting $\sigma_{M_{\text{bol}}}$ are in the range 0.03-0.26 mag. All isochrones were kindly provided by DA Vandenberg. Fig 5a illustrates the effect of a non-LTE correction of +0.2 dex in $[\text{Fe}/\text{H}]$ as inferred from PA Bergbusch & DA Vandenberg's (2000, in preparation) models (see text): the dashed line is a standard isochrone of 12 Gyr ($[\alpha/\text{Fe}] = +0.3$, $Y \simeq 0.24$) with $[\text{Fe}/\text{H}] = -1.54$ (LTE value), and the full lines are isochrones with $[\text{Fe}/\text{H}] = -1.31$ (non-LTE value) of 12 Gyr (upper line) and 14 Gyr (lower line). Fig 5b illustrates the effect of microscopic diffusion of He as inferred from Proffitt's & Vandenberg's (1991) models: isochrones ($[\text{Fe}/\text{H}] = -1.3$ and $[\text{O}/\text{Fe}] = 0.55$), of 12 Gyr with (full line) and without (dashed-line; upper line 12 Gyr, lower 14 Gyr) microscopic diffusion are plotted.

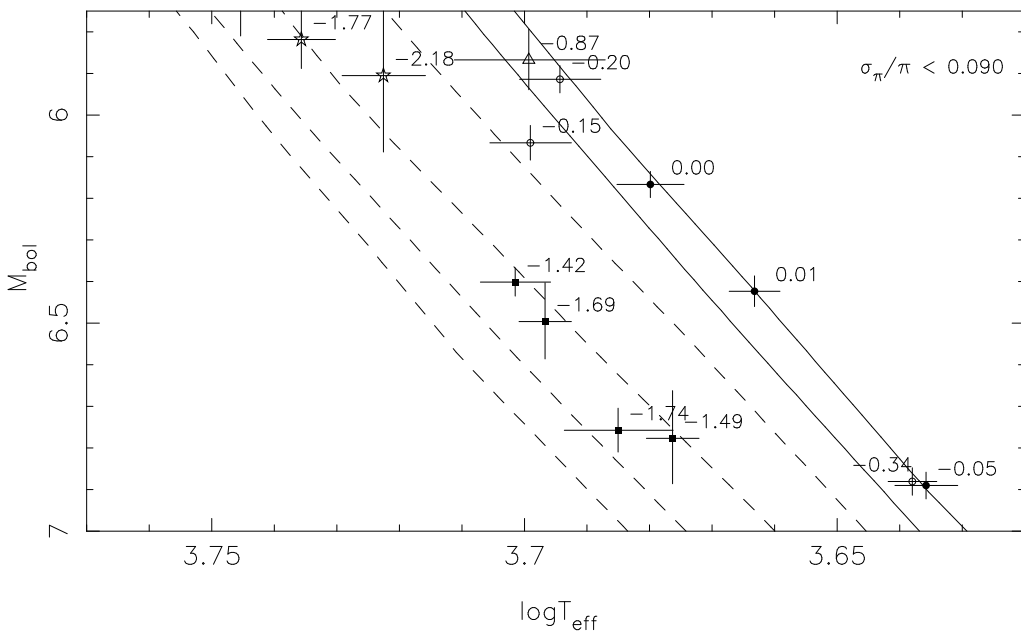


Figure 6: “Hipparcos” H-R diagram of non-evolved stars with $\sigma_{\pi}/\pi < 0.10$. Each star is labeled with its $[Fe/H]$ -value. Standard isochrones are plotted with, from left to right, $[Fe/H]=-2.0, -1.5, -1.0, -0.5, 0.0, 0.3$ (from Lebreton 2000).

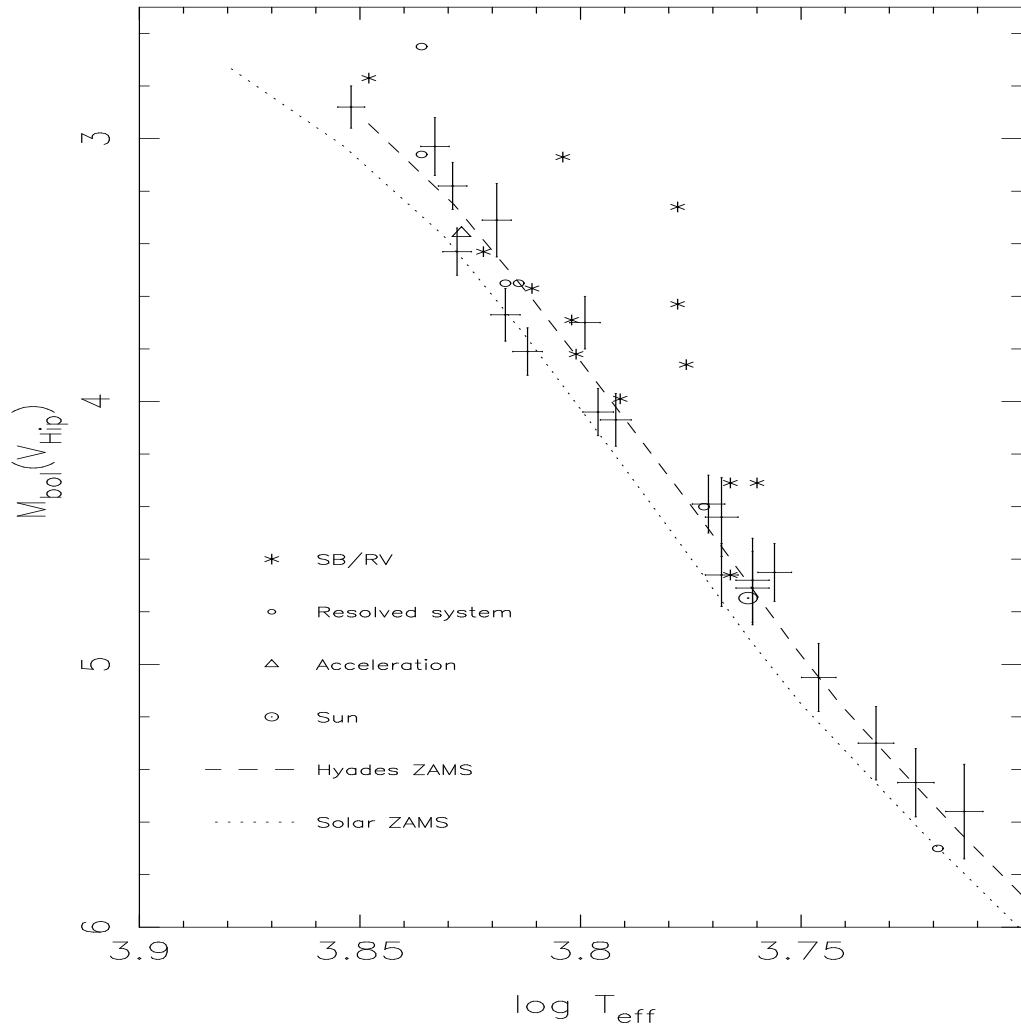


Figure 7: Hipparcos H-R diagram for 40 selected low MS stars in the Hyades. The mean $[\text{Fe}/\text{H}]$ is 0.14 ± 0.05 . Stars with error bars are not suspected to be double or variable. Internal errors on T_{eff} are in the range 50-75 K. Double or variable stars are also indicated: objects resolved by Hipparcos or known to be double systems are shown as circles, triangles denote objects with either detected photocentric acceleration or objects possibly resolved in photometry, and ‘*’ means spectroscopic binary or radial velocity variable. Theoretical ZAMS loci are given for the Hyades (dashed line, $Y=0.26, Z=0.024$) and solar (dotted line, $Y=0.266, Z=0.0175$) chemical compositions (from Perryman et al 1998).

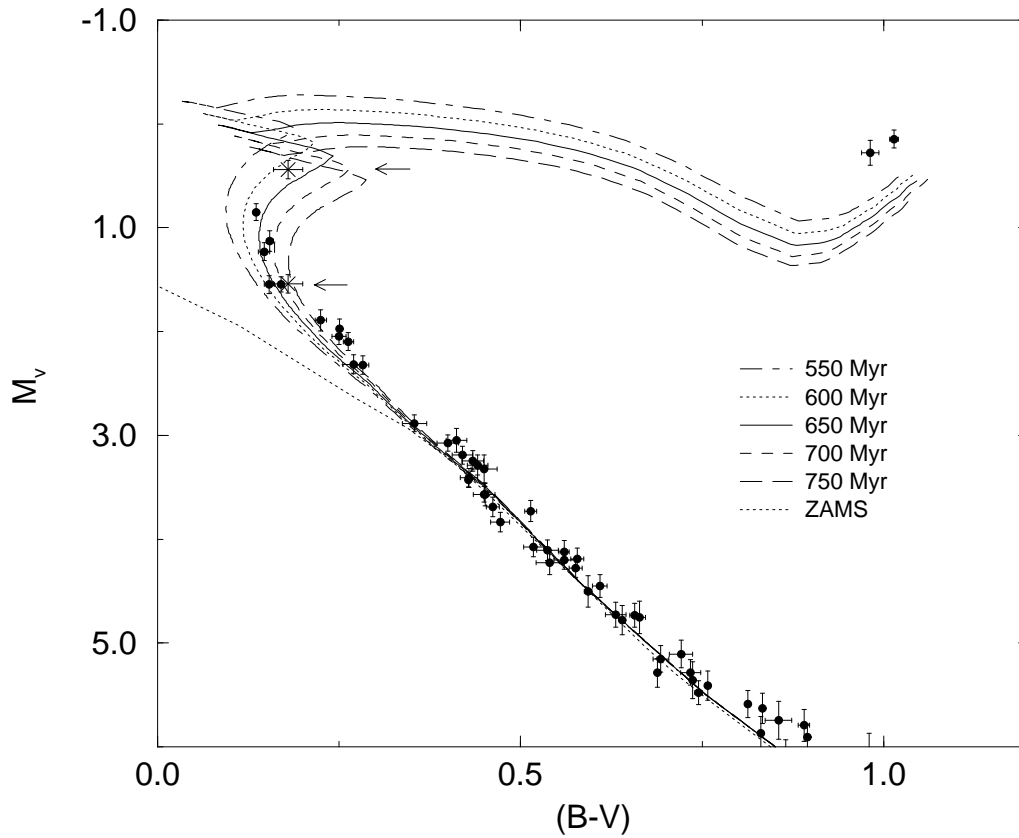


Figure 8: Hipparcos C-M diagram of the Hyades. V and $B-V$ values are from the Hipparcos catalogue ($\sigma_{(B-V)} < 0.05$ mag). The loci of ZAMS and theoretical isochrones calculated with overshooting ($\alpha_{ov} = 0.2$) are indicated. Arrows indicate the position of the components of the binary system θ^2 Tau used for the age determination (from Perryman et al 1998).

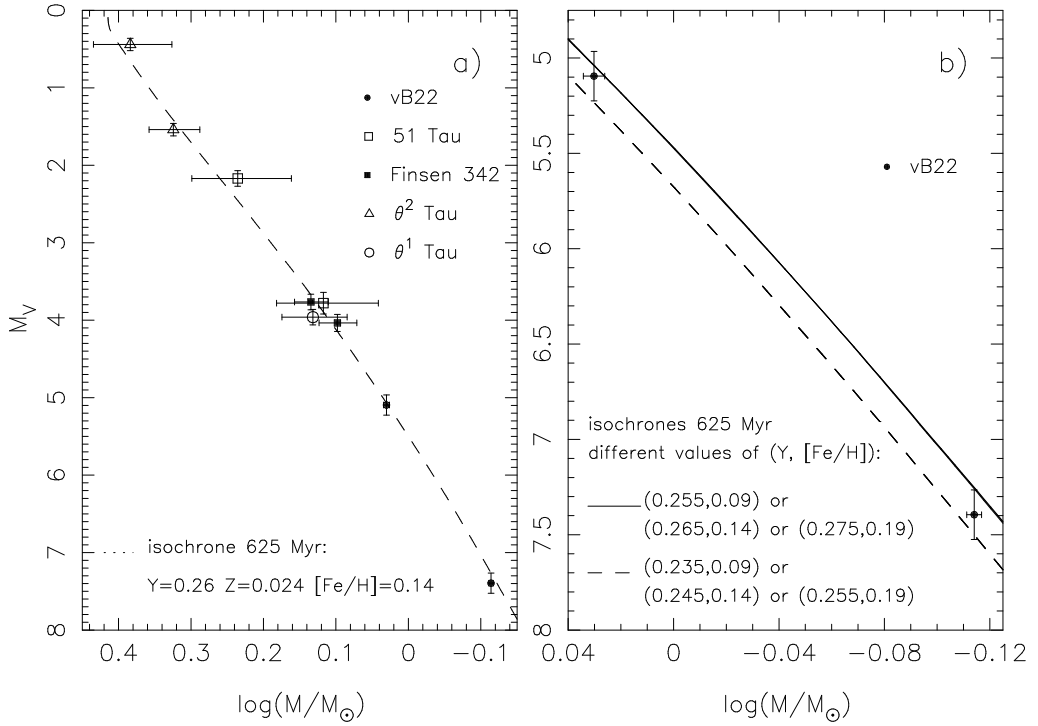


Figure 9: Figure 9a: the Hyades empirical and theoretical mass-luminosity relations. Masses are from Peterson & Solensky (1988, vB22), Torres et al (1997a, b, c, Finsen 342, θ^1 , θ^2 Tau) and Sderhjelm (1999, 51 Tauri from Hipparcos data). The isochrone is for 625 Myr, taken from the same calculations used in Figure 8. Figure 9b illustrates how the precise positions of the members of vB22 allow to discriminate between different $(Y, [\text{Fe}/\text{H}])$ values.